

# Snow and ice in the hydrosphere

# 4

Jan Seibert<sup>a,b</sup>, Michal Jenicek<sup>c</sup>, Matthias Huss<sup>d,e,f</sup>, Tracy Ewen<sup>a,g</sup>, and Daniel Viviroli<sup>a</sup>

*Department of Geography, University of Zurich, Zurich, Switzerland<sup>a</sup> Department of Aquatic Sciences and Assessment, Swedish University of Agricultural Sciences, Uppsala, Sweden<sup>b</sup> Department of Physical Geography and Geoecology, Charles University, Prague, Czech Republic<sup>c</sup> Laboratory of Hydraulics, Hydrology and Glaciology (VAW), ETH, Zurich, Switzerland<sup>d</sup> Department of Geosciences, University of Fribourg, Fribourg, Switzerland<sup>e</sup> Swiss Federal Institute for Forest, Snow and Landscape Research (WSL), Birmensdorf, Switzerland<sup>f</sup> Department of Computer Science, ETH Zurich, Zurich, Switzerland<sup>g</sup>*

---

## Abstract

In large areas of the world, runoff and other hydrological variables are controlled by the spatial and temporal variation of the 0 °C isotherm, which is central for the temporal storage of precipitation as snow or ice. This storage is of crucial importance for the seasonal distribution of snow and ice melt, a major component of the movement of water in the global water cycle. This chapter provides an introduction to the role of snow and ice in the hydrosphere by discussing topics including snowpack characteristics, snow observation approaches, the energy balance of snow-covered areas, and modeling of snowmelt. Furthermore, the role of glaciers and glacial mass balances, including modeling glacier discharge, is discussed. An overview of the hydrology of snow- and ice-covered catchments is given, and the influence of snow, glaciers, river ice, seasonally frozen soils, and permafrost on discharge is discussed. Finally, the impacts of climate change on snow and ice are discussed.

---

### 4.1 Introduction

Snow and ice are important components of the hydrosphere, and many processes related to snow and ice are dominated by the threshold behavior caused by the large amount of energy, which is released or consumed during the phase change between liquid and frozen water. In the Northern Hemisphere, about one quarter of the area experiences mean annual temperatures below 0°C and for more than half of the area temperatures are below 0°C during at least 1 month of the year (Brown and Goodison, 2005; Davison and Pietroniro, 2005). A permanent or seasonal snow cover occurs in large parts of the world, even if snow cover extent in the Southern Hemisphere is much less (about 2% of that in the Northern Hemisphere) due to smaller land areas. The annual snowfall fraction increases with elevation and latitude, where the amount of solar energy varies significantly over the year. Overall, the climate determines where snowfall typically occurs and drivers at the global, regional, and local scales all play a role. The often small difference in temperature which determines whether precipitation falls as rain or snow can have large effects on ecosystems. In regions where either a permanent or seasonal snow

cover exists, snow significantly influences all aspects of the cryosphere and many environmental variables as well as social and economic patterns.

The existence of snow cover on the ground immediately changes the partitioning of the incoming energy. Snow has a high albedo, which means that a large fraction of the incoming solar energy is reflected back into the atmosphere. The albedo of new snow can be up to about 0.9 and decreases to about 0.5 as snow ages, whereas typical values for areas without snow cover are 0.1–0.3 (Table 4.1). This difference explains the observation that mean air temperatures are significantly lower ( $\sim 5^{\circ}\text{C}$ ) if the ground is covered by snow, which implies that there is a positive feedback that can enhance the accumulation of snow in early winter and maintain the snowpack longer into late spring and summer.

Snow also has a high insulation capacity, which means that energy fluxes between the atmosphere and the ground are significantly reduced by snow. It has, for instance, been observed that seasonal soil freezes to deeper depths if there is no snow present compared to the situation with an insulating snow cover (Hayashi, 2013). Wintertime snowpack also acts as insulation for the local environment, providing an insulating cover for vegetation and hibernating animals.

The spatial and temporal variation of the  $0^{\circ}\text{C}$  isotherm is central for the temporal storage of precipitation as snow or ice. This storage is of crucial importance for the seasonal distribution of snow and ice melt, a major component of the movement of water in the global water cycle. In many areas, snow and ice melt are the main contribution to annual river runoff and can affect water supply, hydropower production, agricultural irrigation, and transportation. In extreme cases, large snowmelt rates, sometimes combined with heavy springtime rainfall, may lead to disastrous flooding. Rapid snowmelt can also trigger landslides and mass-wasting of hillslopes. Too little snowmelt, on the contrary, can lead to low river flows in summer, or even drought, which can have significant economic, environmental, and ecological consequences. Especially in many arid regions of the world, the temporal storage of snow in nearby mountainous regions is of critical importance for water supply.

In this chapter, we provide an overview of the role of snow and ice in the water cycle. In the following section on snow accumulation and snowpack properties, we address topics including snowpack characteristics, snow observation approaches, energy balance of snow-covered areas, and modeling of snowmelt. In the section that follows, we discuss glaciers and glacial mass balance, including modeling glacier discharge. In the final section, an overview of the hydrology of snow- and ice-covered catchments is given, and the influence of snow, glaciers, river ice, seasonally frozen soils, and permafrost on discharge is discussed. The present chapter thus mainly provides a background to the other chapters in this volume, which discuss the different aspects of snow- and ice-related natural hazards.

**Table 4.1 Albedo of various surfaces for short-wave radiation (based on Hendriks, 2010; Maidment, 1992).**

Surface	Typical range in albedo [-]
New snow	0.80–0.90
Old snow	0.60–0.80
Melting snow (porous → fine grained)	0.40–0.60
Snow ice	0.30–0.55
Coniferous forest with snow	0.25–0.35
Green forest	0.10–0.20
Bare soils	0.10–0.30
Water	0.05–0.15

## 4.2 Snow accumulation and melt

### 4.2.1 Snowpack description

A snowpack can be described in many different ways. Although snow depths can be easily measured, the snow water equivalent (SWE in mm) is the more relevant property of a snowpack for most snow hydrological questions because the SWE is the water content in the snow that directly contributes to runoff. SWE is defined as the amount of liquid water that would be obtained upon the complete melting of the snowpack per unit ground surface area. SWE [mm], snow depth ( $d$  [m]), snow density ( $\rho_s$  [ $\text{kg m}^{-3}$ ]), and water density ( $\rho_w = \sim 1000 \text{ kg m}^{-3}$ ) are directly related (Eq. 4.1, where  $S_{WE}$  refers to SWE). The density of snow can vary considerably (Table 4.2) (DeWalle and Rango, 2008; Fierz et al., 2009; Maidment, 1992; Singh and Singh, 2001). New snow usually has the lowest densities with about  $100 \text{ kg m}^{-3}$  and densities increase with aging snow due to metamorphism to about  $350\text{--}400 \text{ kg m}^{-3}$  for dry old snow and up to  $500 \text{ kg m}^{-3}$  for wet old snow. Firn, snow that has not melted during the past summer, has densities typically ranging from  $550$  to  $800 \text{ kg m}^{-3}$ .

$$S_{WE} = 1000 d \frac{\rho_s}{\rho_w} \quad (4.1)$$

Different types of precipitation also impact the density of the snowpack. These include the type of snow (wet or dry), graupel, sleet (or ice pellets), freezing rain, freezing drizzle, rain, and drizzle. The type of snow crystal, determined during the formation by the temperature and moisture content of the atmosphere, also affects the density of the snowpack. The most complex crystal structures tend to form light, low-density snowpacks due to the large spacing in between their branches. Smaller crystals, such as plate crystals, needles, and columns, tend to form heavier, high-density snowpacks because they pack together very efficiently, leaving little space for air pockets in between. Changes in snowpack density due to the increase in pressure of the top layers are caused by the mass of newly fallen snow on the older snow. The increase of snow density causes an increase of thermal conductivity of the snowpack. For further discussion of snow density related to snow microstructure, see Arenson et al. (2021).

At the catchment scale, the amount of snow stored in a catchment is determined by the spatial distribution of SWE, which is largely controlled by the spatial distribution of snow depth. Another important variable is the fractional snow cover. Snow depletion curves describe the SWE as a

**Table 4.2 Typical snow density for different snow types (based on DeWalle and Rango, 2008; Fierz et al., 2009; Maidment, 1992; Singh and Singh, 2001).**

Snow type	Density [ $\text{kg m}^{-3}$ ]
New snow (immediately after falling in calm and very low temperature)	10–30
New snow (immediately after falling in calm)	50–70
Damp new snow	100–200
Settled snow	200–300
Depth hoar	200–300
Wind-packed snow	350–400
Wet snow	350–500
Firn	500–830
Glacier ice	850–917

function of fractional snow cover and are important for forecasting seasonal runoff during the periods with a gradual decrease in snow cover. In alpine areas, the curves are commonly S-shaped, reflecting the area-elevation curve which is typically steep in the low and higher elevations and flatter in the middle elevations (Seidel and Martinec, 2010).

## 4.2.2 Snow accumulation

### 4.2.2.1 Spatial distribution of snow

Large-scale variations of snow accumulation are controlled by temperature, which in turn is related to elevation and latitude (Essery, 2003; Roth and Nolin, 2017) and exposition, whereas at smaller scales the effects of topography on snow redistribution and of forests on snow accumulation and snowmelt can be pronounced. The forest affects snow interception, wind speed, and the density of the snowpack, depending mainly on the type of forest (i.e., coniferous, deciduous, or mixed species), forest age, and canopy cover. The role of the forest is also important during the melting period because it reduces the amount of short-wave solar radiation reaching the surface and thus snowmelt rates (Holko et al., 2009; Jenicek et al., 2018; Jost et al., 2009; López-Moreno et al., 2008; Malle et al., 2019).

Stähli and Gustafsson (2006) evaluated the effect of forests on snow accumulation in a small pre-alpine catchment in Switzerland. They found that as a long-term average, annual maximum SWE was about 50% less in the forest than in open areas. The importance of this effect decreased with increasing snowfall. They also found that the variability of SWE increased throughout the winter season and could be explained by varying snow accumulation and melt at different altitudes and exposures. Similar findings were obtained in several paired catchment studies after clear-cutting. For a catchment in northern Sweden, for instance, it was observed that SWE increased after clear-cutting by about 30% at the end of the accumulation period, snowmelt occurred earlier and spring flood runoff increased significantly in some years (Schelker et al., 2013). Overall, clear-cutting increases the snowpack and SWE directly since snow is no longer intercepted by the vegetation canopy. Clear-cutting will also have a local effect on the wintertime energy budget through an increase in albedo.

### 4.2.2.2 Snow observations

Snowfall can be measured by precipitation gauges in the same way as rainfall, but the errors due to wind effects are often significant and systematic underestimates of 50% or more have been reported (Rasmussen et al., 2012; Sevruk et al., 2009). Adaptations of precipitation gauges to improve snowfall measurements include heated gauges, which melt the snow and allow the SWE of the snowfall to be measured directly, or gauges with large inverted cone shields that can improve measurements in open, windy areas. Without heating, snowfall often accumulates on top of the gauge, resulting in erroneous measurements (Fig. 4.1). Unlike rainfall, snow remains on the ground and can also be measured in situ. Modern methods for snow depth measurements also contribute to a more accurate estimation of winter precipitation (Helffricht et al., 2018).

Snow depth, either the entire snowpack or the amount of newly fallen snow, is usually measured using a snow stake, which is simply a height measurement taken at the snow surface with the zero points either at the ground surface or last snow layer. Snow depth can also be measured using automatic sensors which usually apply an ultrasonic beam reflecting from ground level. For low-cost measurements carried out in many different localities, time-lapse photography can be used (Garvelmann et al., 2013; Revuelto et al., 2016). This solution enables not only snow depth to be measured but it also

**FIG. 4.1**

Non-functioning precipitation gauge after heavy snowfall (Dannemora, Sweden).

*Photo: Jan Seibert.*

allows information about site conditions during the observing period to be recorded, such as rain-on-snow events, cloudiness, and snow interception on the canopy.

The SWE can be measured directly by taking a snow core with a snow tube, and then weighing the snow and dividing by the area of the opening of the snow tube. As an alternative, the SWE can be computed from the measurements of snowpack depth ( $d$  [m]) and estimates of snow density ( $\rho_s$ ) using Eq. (4.1) and the density of liquid water ( $\sim 1000 \text{ kg m}^{-3}$ ). Since snow depth generally varies spatially more than snow density and is also easier to measure, it is usually a good strategy to measure snow depth at a frequency at least 10 times greater than snow density. Statistical estimation methods of snow density and its evolution during the winter can be used in cases where only snow depth data are available (Jonas et al., 2009). Such approaches often give similar results to more complex physically based modeling of SWE (Bavera et al., 2014).

For continuous SWE measurements, a snow pillow or snow scales are often used (Fig. 4.2). Such observations are based on measuring the mass of the snow lying on the installed pillow or sensor plate with a specific area (usually  $9 \text{ m}^2$ ). Another way of measuring SWE in situ is a snow permittivity measurement of the snowpack (Egli et al., 2009). This measurement is based on measuring the dielectric constant of three main components of the snowpack: ice, water, and air. The measurement is carried out along a ribbon placed in the snowpack (usually placed parallel or diagonal to the ground). With this system, it is possible to measure SWE, snow density, and liquid water content. Another way to acquire combined information of snow depth, SWE, and liquid water content is to measure a GPS signal which is attenuated and delayed in the snowpack, dependent on its water content (Koch et al., 2019).

Mapping SWE over larger areas remains challenging, especially for mountainous regions (Dozier et al., 2016). However, new satellite missions (Bormann et al., 2018) or the combination of remote sensing with volunteered geographic information (including the upload of geotagged photos) and modeling (Dong, 2018) provides new opportunities for better spatial data coverage. Promising results have also been achieved using ground-based or airborne ground-penetrating radar (Bühler et al., 2015; Lundberg et al., 2006; Sold et al., 2013). An alternative is the measurement of gamma radiation from

**FIG. 4.2**

Climate station with snow scales in Modrava, Czech Republic (*left*), and snow pit close to Furka Pass, Switzerland (*right*).

*Photo: Michal Jenicek.*

the earth (Peck et al., 1971). The method is based on the attenuation of natural gamma radiation by the water accumulated in the snowpack with a detector fixed either a few meters from the ground surface or read from an aircraft. Gamma radiation is then measured over time with and without snow cover. A more recent technique is the highly accurate remote sensing of the snowpack on the ground and on glaciers using laser scanners (Egli et al., 2012; Grünwald et al., 2010; López-Moreno et al., 2015; Prokop, 2008; Sold et al., 2013). Sensors can be placed in the aircraft (LIDAR) or can be used as a terrestrial device placed on the tripod (terrestrial laser scanning, TLS). Due to their construction and method of use, scanners have enabled the remote sensing of areas that are impossible to measure directly; for example, distant locations or steep slopes prone to ice or snow avalanches or rock falls (Egli et al., 2012; Grünwald et al., 2010). Present sensors are highly accurate (<1 cm both horizontally and vertically). However, not all sensors can be used for snow sensing due to the reflection properties of the snow cover (Prokop, 2008). Because of the high acquisition cost of laser scanners, a laser range finder is sometimes used to determine the snow depth (Hood and Hayashi, 2010). The disadvantages of these devices are mainly: (1) poorer resolution of the snow depth grid, (2) usually only a small area can be covered from one location, and (3) measurements take more time than with a terrestrial laser scanner. Despite these disadvantages, the device is highly portable and a potentially improved alternative to expensive laser scans. The combination of different approaches and data assimilation might be a promising way toward better SWE estimates (Painter et al., 2016; Smyth et al., 2019).

In recent years, much progress has been made using remote airborne- and spaceborne-sensing methods to determine snow characteristics, snow depth, and avalanche dynamics (Bühler et al., 2015; Eckerstorfer et al., 2016; Molotch and Margulis, 2008; Tait, 1998; Vander Jagt et al., 2013). Methods for remotely determining the SWE based on the repeated monitoring of snow cover area

(SCA) have been developed (Farinotti et al., 2010; Molotch and Margulis, 2008). SCA can be measured both by optical and radar instruments. Radar is also suitable for observations of other parameters such as the amount of liquid water content (Storvold et al., 2006) and passive microwave sensors can also be used to derive SWE (Molotch and Margulis, 2008; Tait, 1998). Miniaturization of sensors has also enabled an explosive application of small platforms, such as unmanned aerial systems (UAS) used to carry, for example, optical cameras, multispectral cameras, or laser scanners (Bühler et al., 2016; De Michele et al., 2016; Jagt et al., 2015; McCabe et al., 2017). Such systems enable high-precision retrieval of the snow depth at local scales and also help to assess the role of environmental factors, such as vegetation, which influences spatial and temporal snow distribution (Lendzioch et al., 2019).

### 4.2.3 Snow redistribution, metamorphism, and ripening process

#### 4.2.3.1 Snow redistribution by wind

Snow transport, or the deposition of falling snow, is controlled by the wind field of the surface boundary layer, which is modified (in speed and direction) by local surface topography (Lehning et al., 2008). Variability in the wind field ultimately causes snow to be non-uniformly distributed or redistributed over the landscape. Therefore, it is difficult to simulate this process correctly using catchment hydrological models (Freudiger et al., 2017). The spatial variation of SWE is commonly strongly influenced by the effects of topography on snow redistribution, and the timing of the snow's disappearance is in turn controlled by this redistribution in addition to differences in melt rates (Anderton et al., 2004) (Fig. 4.3). The spatial redistribution of snow affects the basin-averaged snowmelt to different degrees;

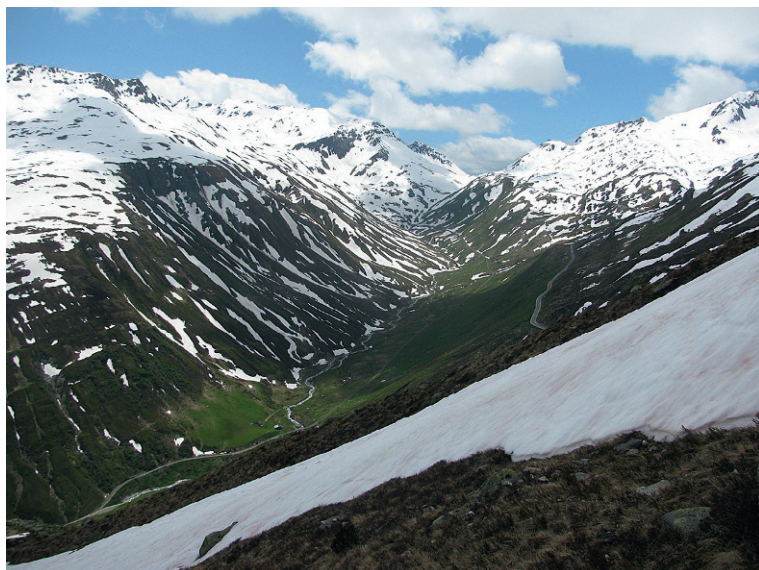


**FIG. 4.3**

Spatial distribution of snow as a result of varying snow accumulation and melt and snow redistribution (Furka Pass, Switzerland, June 2013). Snow at the south-facing side of the valley had already melted, whereas on the north-facing side snow was still present in areas that had gained snow due to snow redistribution.

*Photo: Jan Seibert.*

the effects of snow redistribution were found to be very important for Reynolds Creek (Idaho, USA; Luce et al., 1998), whereas only local effects were reported for an area in the German Alps (Bernhardt et al., 2012). For Reynolds Creek, the spatial redistribution of snow in drifts sustained streamflow later into the spring and summer compared to a more uniform snowpack.

#### **4.2.3.2 Snow metamorphism**

The process of snow crystal metamorphism begins immediately after snowpack accumulation on the ground. In nature, most crystal changes are related to pressure and temperature changes in the snowpack (DeWalle and Rango, 2008). The three main types of snowpack metamorphism are briefly discussed later (see the chapter by Arenson et al., 2021 for a discussion of metamorphism in the context of snow microstructure).

Equi-temperature metamorphism is based on the migration of vapor from convex to concave ice surfaces because of higher vapor pressure on convex surfaces of the crystals than on concave surfaces. Snow crystals become more rounded due to this process. More rounded crystals increase snowpack stability due to their higher compaction ability and thus reduce the risk of avalanches.

Temperature-gradient metamorphism occurs as a result of changes in snowpack temperature and is the most important pre-melt densification process for the snowpack. The physical principle is based on the higher vapor pressure in a warmer snowpack than in a cooler snowpack. This gradient causes an upward migration of water vapor within the snowpack, from the warmer ground surface to the cooler snow surface. This process causes the formation of a new layer with large faceted crystals (depth hoar) which are poorly connected to each other and thus snowpack stability on the slope is lower and more prone to avalanches (e.g., Fierz et al., 2009). This depth hoar layer can be recognized only by snow pit analysis, which is infrequently carried out due to the time and effort required, and thus represents a potential danger.

Melt-freeze metamorphism is typical during the spring period when air and snowpack temperatures increase due to the higher solar radiation. Snow on the surface of the snowpack tends to melt first, typically the small snow grains since they have lower melt temperatures compared to large snow grains. The melted snow can trickle into the colder middle portion of the snowpack where it refreezes and leads to the formation of a well-connected large-grained snowpack. A specific amount of liquid water is usually present in the snowpack before snowmelt; typically from 2% to 5% with a maximum of 10% (see, e.g., Fierz et al., 2009; Techel and Pielmeier, 2011). A higher portion of liquid water can lead to the specific type of snow and water movement called slush flow which often also activates a topsoil layer (Eckerstorfer and Christiansen, 2012). Melt-freeze metamorphism usually increases snowpack stability. On the contrary, the avalanche danger increases with an increase in the volume of liquid water stored in the snowpack. For an in-depth discussion on snowpack stability and avalanches, the reader is referred to Schweizer et al. (2021).

#### **4.2.4 Snowpack development**

In regions where there is a seasonal snowpack, the snowpack develops over the course of the season starting with an accumulation phase, when precipitation falling as snow accumulates, increasing the SWE until the melt period begins with an increased input of solar radiation. At first, the melt is characterized by a warming phase, when the average snowpack temperature increases more or less steadily until the snowpack becomes isothermal, that is, when the temperature over the snow profile reaches 0°C. At this point, melting within the snowpack is possible and marks the beginning of the ripening

phase. The melt within the snowpack is retained until the liquid water holding capacity is exceeded. Once exceeded, any further input of energy (from warmer air and/or soil and/or liquid precipitation) gained by the snowpack will then be used for phase changes from solid to liquid, producing more melt. The output phase begins when water output occurs at the base of the snowpack. It is important to note that a snowpack, as a porous medium, can store considerable amounts of liquid water. As a rule of thumb, snow can hold up to about 10% of the snowpack SWE by capillary forces against gravitation.

#### 4.2.4.1 Cold content

The cold content of a snowpack is the total heat which is necessary to warm the snowpack to 0°C over the entire vertical profile and can be expressed as the amount of liquid water (in [mm]) which must be frozen in the snowpack to warm the snowpack to isothermal conditions (DeWalle and Rango, 2008). This variable of the energy state of a snowpack is important for snowmelt processes and their modeling and can be calculated as:

$$C_C = 1000 \frac{\rho_s \cdot c \cdot d \cdot (273.16 - T_s)}{\rho_w \cdot L_f} \quad (4.2)$$

where  $C_C$  is the snowpack cold content [mm],  $\rho_s$  is the snowpack density [ $\text{kg m}^{-3}$ ],  $c_i$  is the specific heat of ice [ $\text{J kg}^{-1} \text{K}^{-1}$ ],  $d$  is the snowpack depth [m],  $T_s$  is snowpack temperature [K],  $\rho_w$  is the water density [ $\text{kg m}^{-3}$ ], and  $L_f$  is the latent heat of fusion [ $\text{J kg}^{-1}$ ].

Cold content is often used by hydrologists when simulating snowmelt runoff. Generally, it can be calculated for the full profile or for specific snowpack layers, which is useful for modeling avalanches. The evolution of the snowpack and snowpack temperatures in specific layers can be used to calculate the cold content over the accumulation and melt periods (Fig. 4.4).

### 4.2.5 Snowmelt

#### 4.2.5.1 Energy balance

The development of the snowpack depends on the amount of energy available to the snowpack for melting snow which can be expressed in terms of the snowmelt energy balance. The energy balance of the snowpack represents the basic approach to snowmelt modeling and calculates all heat fluxes between the atmosphere, snow, and soil (Fig. 4.5). The snowmelt energy balance can be defined by:

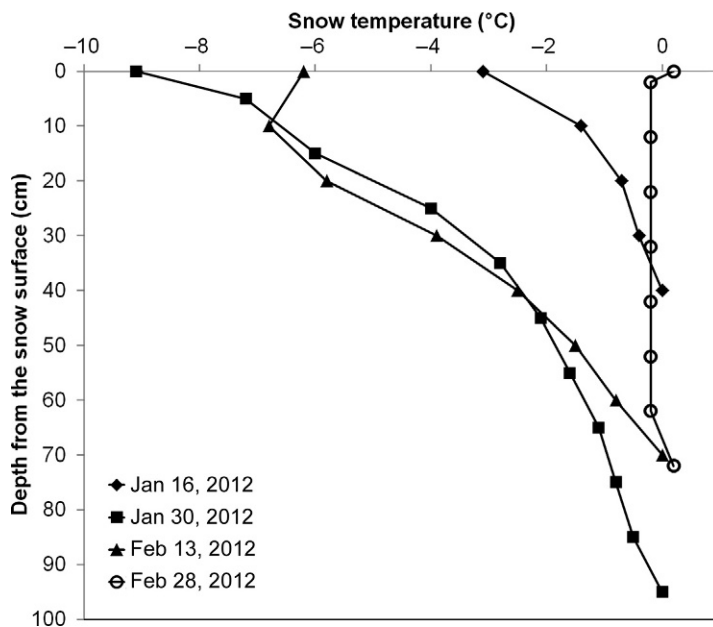
$$Q_m = Q_{ns} + Q_{nl} + Q_h + Q_e + Q_p + Q_g + Q_i \quad (4.3)$$

where all  $Q$  refer to heat fluxes [ $\text{W m}^{-2}$ ].  $Q_m$  is the total heat flux (positive or negative) available for snow melting,  $Q_{ns}$  is the heat flux due to short-wave radiation,  $Q_{nl}$  is the heat flux due to long-wave radiation,  $Q_h$  is the sensible heat flux,  $Q_e$  is the latent heat flux caused by water phase changes,  $Q_p$  is the heat supplied by precipitation,  $Q_g$  is the heat supplied by the ground, and  $Q_i$  is the change in the internal energy of the snowpack.

The short-wave and long-wave radiation balances of the snowpack  $Q_{nr}$  can be computed according to

$$Q_{nr} = (I - \alpha) \cdot S_i + (L_i - L_o) \quad (4.4)$$

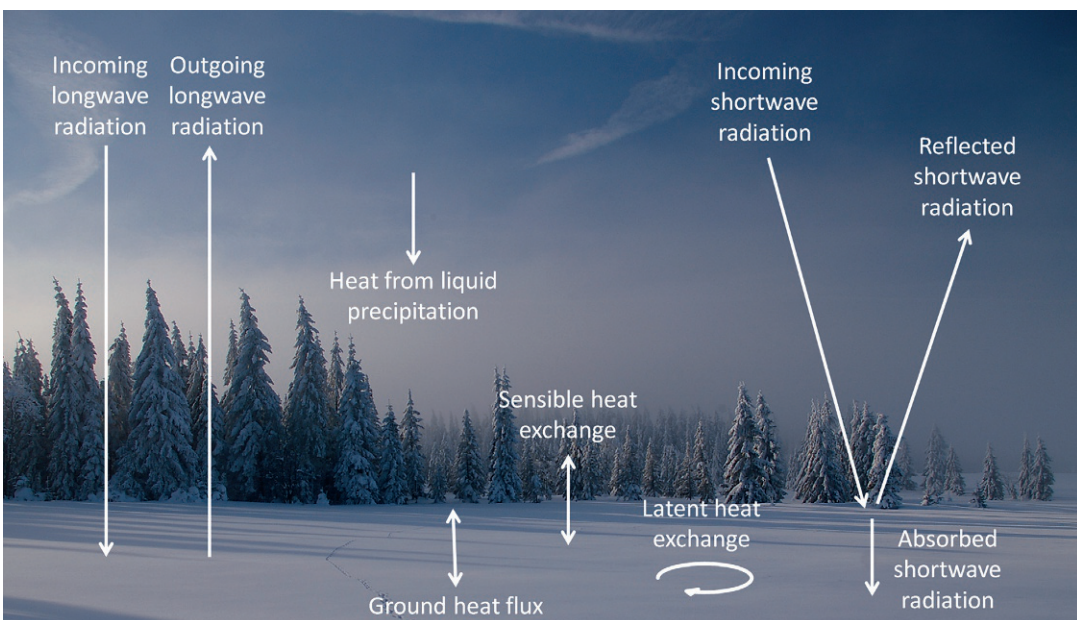
where  $Q_{nr}$  [ $\text{W m}^{-2}$ ] is the total radiation,  $\alpha$  [–] is the albedo,  $L_i$  is the incoming long-wave radiation,  $L_o$  is the outgoing long-wave radiation, and  $S_i$  is the incoming short-wave radiation (all in  $\text{W m}^{-2}$ ) (Singh and Singh, 2001). The amount of short-wave radiation absorbed by snow depends mainly on latitude,



**FIG. 4.4**

Snow temperature evolution in a snow pit during the winter 2011/2012; Krušné Mountains, Czech Republic (data from Charles University in Prague, Faculty of Science). The first two dates represent typical winter conditions with low air temperatures. The third date, Feb 13, 2012, represents the beginning of spring warming (see snow temperature inversion in top 10cm of the snowpack). The last date, Feb 28, 2012, represents isothermal conditions in the snowpack during the snowmelt.

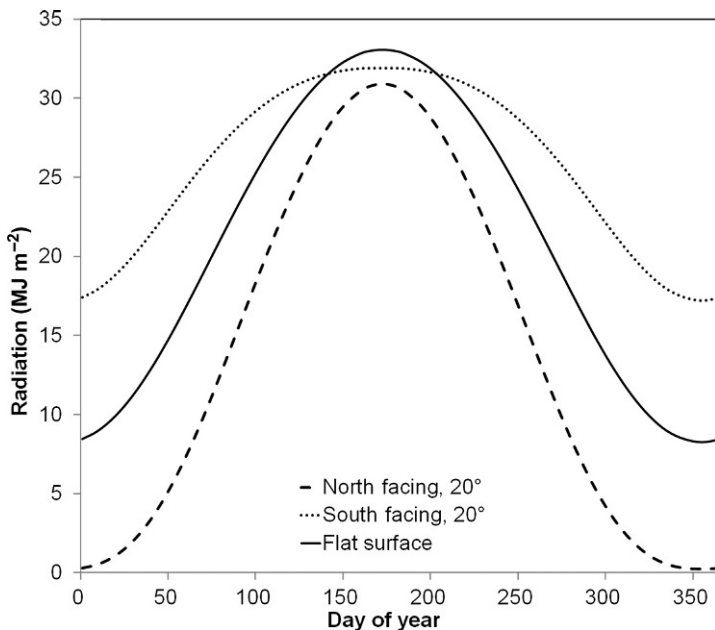
*Data from Charles University in Prague.*



**FIG. 4.5**

Energy balance of the snowpack. Arrows represent individual heat fluxes and interactions between the atmosphere, snow, and soil environments.

*Photo: Michal Jeníček.*

**FIG. 4.6**

Daily potential solar irradiation for slopes 20° north and south and a flat surface as a function of day of the year (i.e., Julian date) at a latitude of 45°N. The calculation considers clear sky conditions (based on the method presented in Dingman, 2008).

season (sun inclination), atmospheric diffusion, slope, aspect, and obstacles with shadow effects like forest cover (see also Fig. 4.6).

Long-wave radiation (in the range of 6.8–100 µm) is both incoming (from the atmosphere, surrounding terrain, and vegetation) and outgoing from the snow surface (Singh and Singh, 2001). The radiation from the surface is largely absorbed by the atmosphere, mainly by absorption from carbon dioxide and water vapor.

A convective sensible heat transfer between the air and the snow is driven by differences between air and snowpack temperatures. The amount and the direction of the heat flux is given by

$$Q_h = \rho_a \cdot c_{pa} \cdot (T_a - T_s) / r_h \quad (4.5)$$

where  $\rho_a$  is the density of air [ $\text{kg m}^{-3}$ ];  $c_{pa}$ , the specific heat of air at constant pressure [ $1010 \text{ J kg}^{-1} \text{ }^{\circ}\text{C}^{-1}$ ];  $T_a$  and  $T_s$  [ $^{\circ}\text{C}$ ] are the air and snow surface temperatures respectively; and  $r_h$  is a term to describe the resistance to a heat flux between the snow surface and the overlying air [ $\text{sm}^{-1}$ ], which is a function of surface roughness and wind speed. For the sensible heat flux, large differences between the snow surface and air in spring and early summer cause an energy gain of the snowpack. However, the snowpack temperature is often higher than the air temperature during the spring nights and this situation represents a snowpack energy loss.

The latent heat transfer represents the transfer of water vapor between the atmosphere and the snowpack due to water-phase changes, namely evaporation and sublimation. The water vapor flux and its direction are determined by the vapor pressure gradient and the intensity of the turbulence. Evaporation and the sublimation from the snow represent a snowpack energy loss; condensation and the deposition of the water vapor on the snow surface represent a snowpack energy gain. The latent heat flux is given by

$$Q_e = L_v \cdot (\rho_{va} - \rho_{vs}) / r_e \quad (4.6)$$

where  $L_v$  is the latent heat of vaporization ( $2.47 \times 10^6 \text{ J kg}^{-1}$ ),  $\rho_{va}$  and  $\rho_{vs}$  are the vapor densities of air and snow surfaces respectively [ $\text{kg m}^{-3}$ ] and  $r_e$  is a term to describe the resistance to water vapor transport between the air and snow surface [ $\text{s m}^{-1}$ ], which is a function of surface roughness and wind speed.

Liquid precipitation on snow, known as rain-on-snow events, represents an additional heat flux into the snowpack which is caused by the higher temperature of the precipitation compared to the temperature of the snow. The heat supplied to the snowpack equals the difference of snow energy before and after precipitation, once temperature equilibrium is reached. Eq. 4.7 expresses the daily amount of transferred energy  $Q_p$  [ $\text{kJ m}^{-2} \text{ d}^{-1}$ ] depending on the precipitation  $P_r$  [ $\text{mm d}^{-1}$ ] and the temperature difference (Singh and Singh, 2001),

$$Q_p = \frac{\rho_w \cdot c_p \cdot (T_r - T_s) \cdot P_r}{1000} + \rho_w \cdot L_f \cdot P_r \quad (4.7)$$

where  $\rho_w$  refers to the water density ( $\sim 1000 \text{ kg m}^{-3}$ ),  $c_p$  refers to the specific heat capacity of water ( $4.20 \text{ kJ kg}^{-1} \text{ }^\circ\text{C}^{-1}$ ),  $T_r$  is the temperature of liquid precipitation,  $T_s$  is the temperature of the snowpack (both in [ $^\circ\text{C}$ ]), and  $L_f$  is the latent heat of fusion ( $334 \text{ kJ kg}^{-1}$ ). Eq. 4.7 is also valid when the snowpack is below freezing, and the rain freezes within the snowpack ( $L_f > 0$ ).

The total amount of heat from the precipitation is generally quite low in comparison with other heat sources. However, precipitation heat input becomes more important when shorter time steps ( $< 1$  day) are considered. For example, a daily precipitation of  $P_r = 30 \text{ mm}$ , rain temperature of  $T_r = 10 \text{ }^\circ\text{C}$  and snow temperature of  $T_s = 0 \text{ }^\circ\text{C}$ , results in a total heat input of  $1260 \text{ kJ m}^{-2} \text{ d}^{-1}$ , or  $14.6 \text{ W m}^{-2}$ . If we consider the same amount of precipitation falling in 3 h, we obtain  $116.7 \text{ W m}^{-2}$ , which is a significant part of the energy balance for that 3-h period, and is comparable to the amount of global short-wave radiation during the cloudy and rainy days.

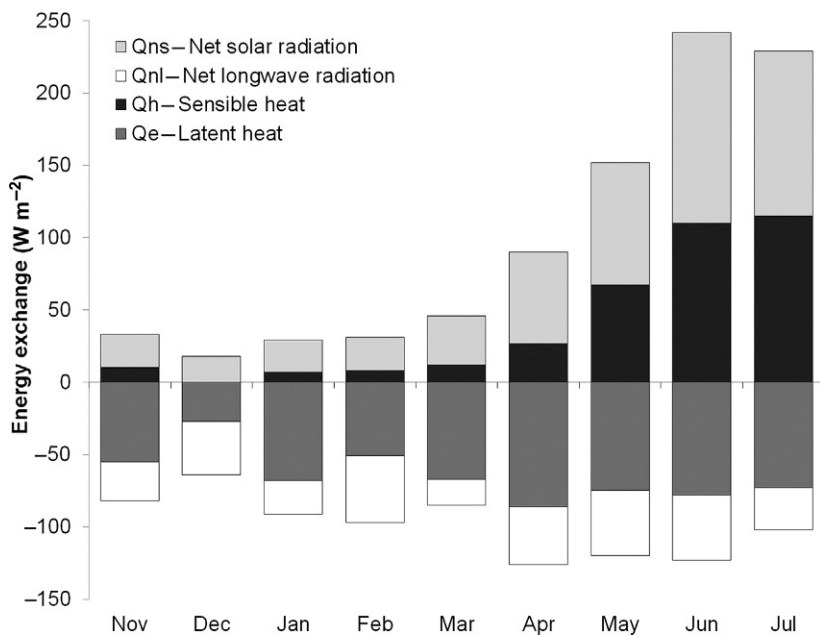
Ground heat flux usually plays a minor role because of the small heat conductivity of the ground and, in the case of a higher snow depth, the lack of solar radiation reaching the soil. The ground heat causes the slow ripening of the snowpack during the winter and may cause slow snowmelt. The ground heat flux can be expressed as

$$Q_g = K_g \cdot \Delta T / \Delta z \quad (4.8)$$

where  $K_g$  is the thermal conductivity of the soil [ $\text{W m}^{-1} \text{ }^\circ\text{C}^{-1}$ ] and  $\Delta T / \Delta z$  [ $^\circ\text{C m}^{-1}$ ] is the temperature gradient in the soil.

The internal energy of the snowpack depends on snow temperature and can be expressed as the sum of the internal energy of the three snowpack components: ice, water, and water vapor. The change of internal energy can play a significant role for glaciers and can delay the onset of melt for snow.

Calculation of the energy balance of the snowpack is a physically based approach for modeling the snowmelt. Based on the availability of meteorological data, a wide range of approximations of the energy balance can be used. The advantage of methods based on the energy budget is their broad range of

**FIG. 4.7**

Seasonal variation in major snowpack energy exchange components at a Sierra Nevada alpine ridge site in 1986. Data from Marks, D., Dozier, J., 1992. Climate and energy exchange at the snow surface in the Alpine Region of the Sierra Nevada: 2. Snow cover energy balance. *Water Resour. Res.* 28, 3043–3054. <https://doi.org/10.1029/92WR01483>.

use under different climatic conditions. The energy budget approach enables snow accumulation, transformation, and melting processes to be physically represented. The main disadvantage of the energy budget method is the difficulty in obtaining the input data necessary for parameterization, calibration, and validation of the model. It is thus difficult to use this approach for calculating snow accumulation and snowmelt for ungauged catchments. Fig. 4.7 (Marks and Dozier, 1992) shows an example of the seasonal variation in the major snowpack energy exchange components.

Energy fluxes can be converted into an amount of melted snow, as described in DeWalle and Rango (2008), that is

$$M = 1000 \cdot Q_m / (\rho_w \cdot L_f \cdot B) \quad (4.9)$$

where  $M$  [ $\text{mm d}^{-1}$ ] is the amount of meltwater,  $Q_m$  [ $\text{kJ m}^{-2} \text{d}^{-1}$ ] is the positive daily output from the energy budget,  $\rho_w$  is the water density ( $\sim 1000 \text{ kg m}^{-3}$ ),  $L_f$  is the latent heat of fusion ( $334 \text{ kJ kg}^{-1}$ ), and  $B$  [–] is the thermal quality of snow, which is defined as the energy necessary to melt a certain mass of snow relative to the energy necessary to melt the same mass of ice at  $0^\circ\text{C}$ .

#### 4.2.5.2 Degree-day method

The calculation of the individual items of the snowpack energy balance is complex and needs a lot of data that are often not available. To overcome the lack of data, the so-called index methods are often used. These methods calculate the snowmelt using some accessible and easily measurable variable that is often related to the energy balance. The air temperature is usually used because of its high correlation

with snow and glacier melt and availability (Braithwaite and Olesen, 1989). Other studies have also shown the importance of long-wave radiation and sensible heat flux on the energy budget. Both heat fluxes usually provide 75% of the entire energy balance, and the variability of air temperatures has been found to be a suitable proxy for the variability of the energy that is available for snowmelt (Hock, 2003; Ohmura, 2001; Pohl et al., 2006; Sicart et al., 2008). Approaches incorporating air temperature are referred to as temperature-index methods.

In the temperature-index method, the SWE decreases according to the melt,  $M$  [mm d<sup>-1</sup>], and is calculated as

$$M = m_f (T - T_T) \quad (4.10)$$

where  $m_f$  [mm °C<sup>-1</sup> d<sup>-1</sup>] is the melt or degree-day factor,  $T_T$  is the threshold temperature for snowmelt to start, and  $T$  is the mean air temperature (both [°C]). Values for  $T_T$  typically vary from −1°C to 3°C. The degree-day factor usually has values between 1 and 10 mm °C<sup>-1</sup> d<sup>-1</sup> with lower values for forested areas (e.g., Seibert, 1999). The temperature-index method has been developed for a daily time step, but has also been used for shorter or longer time intervals.

The initial storage of meltwater within the snowpack can be conceptualized by a liquid water storage which has to exceed a certain fraction of the SWE before drainage from the snowpack occurs (Lindström et al., 1997). If the temperatures decrease, this liquid water might refreeze, which can be simulated by an equation similar to Eq. (4.10), but with a refreezing coefficient  $c_{FR}$  (Eq. 4.11). This coefficient typically has a value of 0.05. This means that the refreezing is 20 times less efficient than the melt, which reflects the difference that the melt occurs at the snow surface, whereas the refreezing occurs when the liquid water is distributed over the snowpack and mainly insulated against the cold.

$$R = C_{FR} \cdot m_f \cdot (T_T - T) \quad (4.11)$$

The temperature-index method dates back to work by Finsterwalder and Schunk (1887) in a glaciological study in the Alps and is probably still the most widely used snowmelt method among hydrologists. Hock (2003) summarized the advantages of the temperature-index method as: (1) the availability of air temperature data, (2) the relatively simple spatial distribution of the air temperature and its predictability, (3) the simplicity of the computational procedure, and (4) satisfactory results of the model despite its simplicity. Although there are clear advantages of this method, Beven (2001) formulated shortcomings of this method as follows: (1) the accuracy of the method decreases with the increasing temporal resolution and (2) the intensity of the snowmelt has a large spatial variability depending on topographic conditions, mainly slope, aspect, and land cover. This variability is very difficult to express using temperature-index methods.

The shortcomings of the models based on the temperature-index method with daily time steps are apparent mainly in cases where air temperature fluctuations are around the melting point. The mean daily air temperature indicates no snowmelt; however, the positive air temperature which occurs during the day could cause snowmelt (Hock, 2003). In mountain areas, it is necessary to consider the change in air temperature depending on the elevation; therefore, the basin is usually divided into several elevation zones (Essery, 2003).

Several enhanced and spatially distributed temperature-index models have been developed (e.g., Hock, 1999; Pellicciotti et al., 2005), which address some of the shortcomings of the classical degree-day model. In these approaches, the degree-day factor varies as a function of potential solar radiation, and the formulation is closer to the principles of the energy balance.

**Table 4.3 Factors influencing melt factor (based on DeWalle and Rango, 2008).**

Factor	Cause	Influence on melt factor
Seasonal influence	Decrease of cold content and albedo, increase in short-wave radiation and snow density	Melt factor increases
Open area vs. forest	Shading and wind protection	Lower melt factor and its spatial variability in the forest
Topography (slope, aspect)	Variability of short-wave radiation and wind exposure	Higher melt factor on south-facing slopes
Snow cover area	Spatial snowmelt variability	Melt factor decreases in the basin with larger snow cover area
Snowpack pollution	Dust and other pollution causes lower albedo	Higher melt factor
Precipitation	Rainfall supplies sensible heat, clouds decrease solar radiation	Generally, lower melt factor on rainy days due to lower radiation. But precipitation itself causes higher melt factor
Snow vs. ice	Glacial ice has lower albedo than snow	Higher melt factor in glaciated basins
Meteorological conditions for certain air temperature	Higher snowmelt with higher wind speed, higher radiation, or higher moisture for the same temperature	Higher melt factor

The melt factor  $m_f$  is the key parameter in Eq. (4.10) and is influenced by several factors (Table 4.3). Martinec (1975) derived an empirical relation between the melt factor and the snow density as

$$m_f = 11 \frac{\rho_s}{\rho_w} \quad (4.12)$$

where  $m_f$  is the melt factor ( $\text{mm } ^\circ\text{C}^{-1} \text{ d}^{-1}$ ),  $\rho_s$  is the snow density, and  $\rho_w$  is the water density (both [ $\text{kg m}^{-3}$ ]). This equation reflects the tendency for the melt factor to increase in the spring together with an increase in snow density due to the ripening process. Kuusisto (1980) derived an empirical relation between the melt factor and the snow density separately for forest and open areas:

$$\text{forest : } m_f = 0.0104 \rho_s - 0.70 \quad (4.13)$$

$$\text{open areas : } m_f = 0.0196 \rho_s - 2.39 \quad (4.14)$$

Forests cause a decrease in the amount of direct solar radiation that reaches the surface and therefore the snowmelt in periods without precipitation. Different melt factors were derived by Federer et al. (1972) for the northwest of the USA. They experimentally derived the melt factor  $4.5\text{--}7.5 \text{ mm } ^\circ\text{C}^{-1} \text{ d}^{-1}$  for open areas,  $2.7\text{--}4.5 \text{ mm } ^\circ\text{C}^{-1} \text{ d}^{-1}$  for deciduous forests, and  $1.4\text{--}2.7 \text{ mm } ^\circ\text{C}^{-1} \text{ d}^{-1}$  for coniferous forests (approximate ratio 3:2:1). Kuusisto (1980) expressed variations in the melt factor dependent on the relative canopy cover of coniferous forests,  $C_{\text{canopy}}$  [–] with typical values of 0.1–0.7, as

$$m_f = 2.92 - 1.64 C_{\text{canopy}} \quad (4.15)$$

## 4.3 Glaciers and glacial mass balance

### 4.3.1 Glacier mass balance

The glacier mass balance provides information about the amount of water stored or released by a glacier within a given time period (Cogley et al., 2011). The glacier mass budget is often evaluated over hydrological years (1 Oct–30 Sept) and is reported as water equivalent per unit area per year [ $\text{m a}^{-1}$ ]. Mass balance  $b$  [ $\text{m a}^{-1}$ ] at one point on the glacier surface is defined as the sum of accumulation  $c$  [ $\text{m a}^{-1}$ ] and ablation  $a$  [ $\text{m a}^{-1}$ ] as

$$b = c + a \quad (4.16)$$

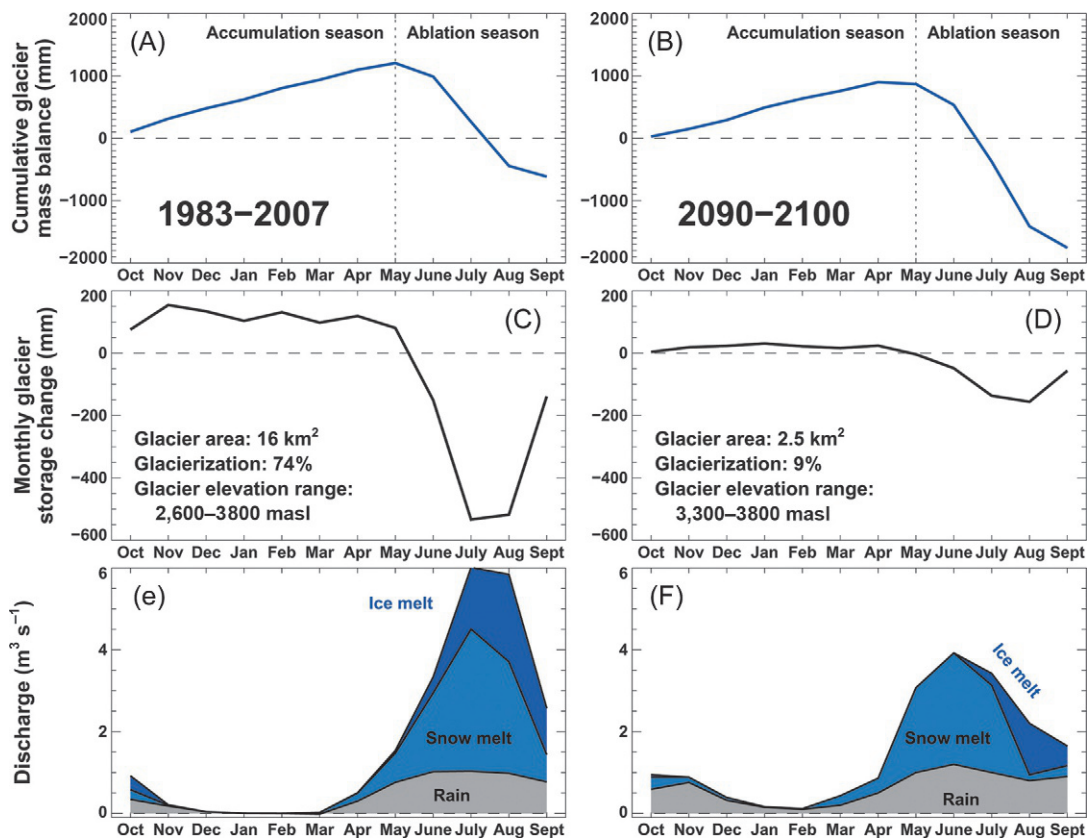
By integrating  $b$  over the glacier surface  $S$  (Cogley et al., 2011), the glacier-wide surface mass balance  $B_{\text{sfc}}$  corresponding to the mean thickness of the water equivalent added or removed can be calculated as

$$B_{\text{sfc}} = \frac{1}{S} \int_S b dS \quad (4.17)$$

Basal ice melt and mass loss due to frontal ablation (calving, ice break-off) add to the total mass balance  $\Delta M$ , but these components are comparatively small or almost negligible for most glaciers in mid- and low-latitude mountain ranges.

Mass balances can be determined using a variety of methods ranging from direct measurements on the glacier surface to techniques using remote sensing. The measurement of glacial mass changes at annual to seasonal timescales has until recently mostly been based on the glaciological method applying spatial interpolation and extrapolation of melt and accumulation measurements at a number of ablation stakes and snow pits (Beedle et al., 2014; Kaser et al., 2003; Østrem and Stanley, 1969; Zemp et al., 2013). At timescales of a few years to several decades, the comparison of repeated information on glacier surface elevation from photogrammetry, radar, or laser scanning, provides accurate data on long-term volume changes of large and inaccessible glaciers (e.g., Berthier et al., 2016; Bolch et al., 2013; Paul and Haeberli, 2008) and nowadays even at regional to global scales (Brun et al., 2017; Dussaillant et al., 2019; Kääb et al., 2012; Zemp et al., 2019). Recently, the application of satellite-based changes in the earth's gravity field has become increasingly popular for evaluating glacier mass changes for entire mountain ranges (e.g., Gardner et al., 2013; Shean et al., 2020; Wouters et al., 2019). The recent advances in satellite-based methods to quantify glacier mass balances have opened incredible opportunities for global assessments of glacier changes.

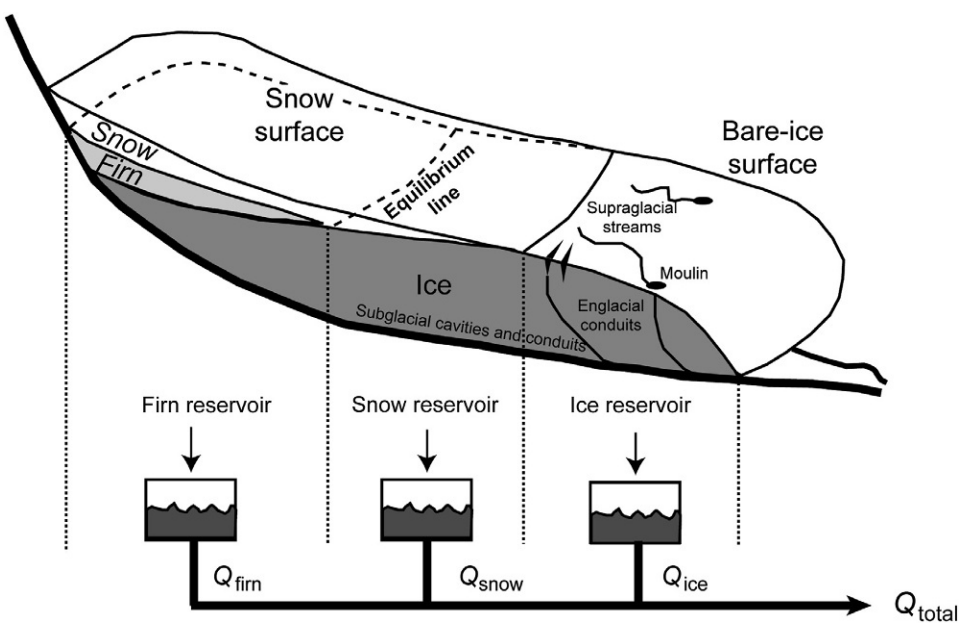
Most mid- and high-latitude mountain glaciers exhibit clearly separated accumulation and ablation periods (Fig. 4.8A). Glacier storage changes are positive during the winter season with precipitation mainly falling as snow and limited or absent melt. The ablation season is often concentrated into a few months with the highest air temperatures and strong solar radiation (Fig. 4.8C). Glaciers thus store most of the winter precipitation, which is often strongly enhanced due to orographic uplift, and release it during a few summer months (Jansson et al., 2003; Stenborg, 1970). This behavior has a significant effect on the hydrological regime of glacierized drainage basins, which are dominated by the components of snow and ice melt (Fig. 4.8E).

**FIG. 4.8**

Glacier mass balance  $B_{sfc}$ , monthly glacier storage change, and runoff components in the catchment of Findelengletscher, Switzerland, for the periods 1983–2007 and 2090–2100 based on glacio-hydrological modeling (Huss et al., 2014). (A and B) Cumulative glacier surface mass balance indicating limited mass losses in 1983–2007 and strongly negative mass balance in 2090–2100. (C and D) Monthly glacier storage change relative to the water balance of the entire catchment. (E and F) Simulated components of catchment discharge (bare-ice melt, snowmelt, and rain minus evapotranspiration).

### 4.3.2 Glacial drainage system

Glaciers are an important storage element in the hydrological cycle and are characterized by their water retention potential at different temporal and spatial scales (Jansson et al., 2003). Whereas water retention in the ice volume refers to the periods of decades to centuries, en- and subglacial water storage is highly important at shorter timescales of a few hours to days. Meltwater derived from bare-ice surfaces is often collected in supraglacial streams and is transported relatively rapidly to a moulin-connecting surface water flow with the glacier bed (Fig. 4.9). Melt generated in the accumulation area, however,

**FIG. 4.9**

Schematic representation of the glacial drainage system and the approach to modeling it using linear reservoirs.

*Redrawn after Hock, R., Jansson, P., 2005. Modeling glacier hydrology. In: Anderson, M.G. (Ed.), Encyclopedia of Hydrological Sciences. John Wiley and Sons: Chichester, UK, pp. 1–9.*

infiltrates into porous firn and snow where it might be stored between days to months until it runs off, or where it refreezes again.

The characteristics and the development of the en- and subglacial drainage system determines water flow through the ice (see [Fountain and Walder, 1998](#), for a review), as well as the hydraulic head within the glacier. Englacial water pressure exhibits a strong connection with surface ice flow over its close link to basal sliding (e.g., [Iken and Bindschadler, 1986](#)). Subglacial water flow occurs either in a rather inefficient, distributed, and interlinked system of small cavities or in individual channels at the ice-bedrock interface that promote an efficient drainage (e.g., [De Fleurian et al., 2018](#); [Flowers, 2002](#); [Röhlisberger and Lang, 1987](#); [Fig. 4.9](#)). The subglacial drainage system develops throughout the melting season with sustained high meltwater input and water pressures. Consequently, the water retention capacity of a glacier decreases with time ([Hewitt et al., 2012](#); [Hock and Hooke, 1993](#)) and the diurnal amplitudes of runoff increase over the summer ([Fig. 4.10](#)). Quantitative knowledge about the properties of the glacial drainage system and its state of evolution can be gained, for example, by dye-tracing experiments (e.g., [Finger et al., 2013](#); [Miles et al., 2019](#); [Werder and Funk, 2009](#)).

### 4.3.3 Modeling glacier discharge

Over the last few decades, many different approaches to simulate glacier discharge have been developed. They focus on the spatiotemporal evolution of the englacial and subglacial drainage system, the water retention capacity of glaciers, as well as on the long-term hydrological impacts of glaciers and

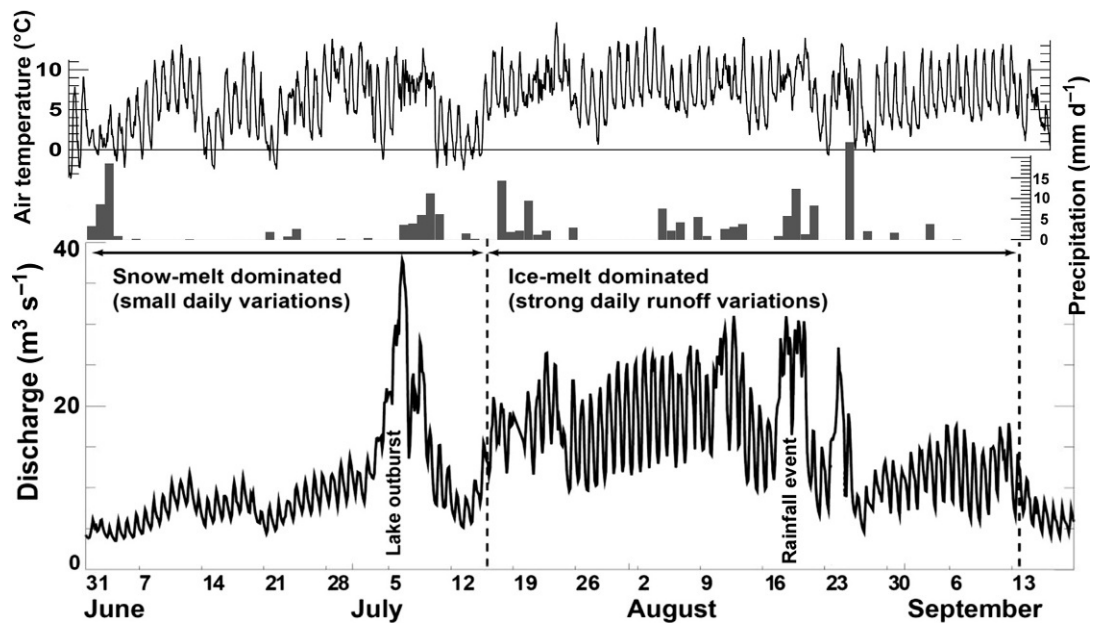


**FIG. 4.10**

Runoff from the catchment of Gornergletscher (66% glacierized), Switzerland, between June and September 2004. Temperature and precipitation series of a station close to the glacier are shown for comparison. The runoff peak in July is driven by the outburst of the glacier-dammed lake. Two runoff peaks in August can be attributed to rainfall events.

their changes (Hock, 2005; Hock and Jansson, 2005). In the following, a brief overview of some modeling approaches is provided. Note that several of the approaches discussed previously in the section on snowmelt also apply to glaciers.

The physically based modeling of the subglacial drainage system has been attempted by a number of studies (e.g., Flowers, 2002; Hewitt et al., 2012; Irarrázaval et al., 2019; Schoof, 2010). By describing the processes of water-cavity growth and drainage-channel enlargement as functions of time-variable water pressure, water supply, the thermodynamic conditions, and the ice flow, the development of the drainage system in time and space can be simulated and the properties of subglacial water flow can be inferred. Many hydrological studies, however, apply simpler, empirical approaches that estimate water retention and glacial runoff using linear reservoir models (Hock and Jansson, 2005). In this widely applied approach, discharge  $Q$  for each time step  $t$  is obtained from a linear relation with the volume  $V$  of hypothetical reservoirs for meltwater originating from snow, firn, and bare-ice surfaces (Hock and Noetzli, 1997, Fig. 4.9) as:

$$Q(t) = k V(t) \quad (4.18)$$

The retention constant  $k$  is characterized by the water retention capacity of the respective reservoir and is determined by calibrating the model with field data (see, e.g., Hock, 1999).

The modeling of glacier hydrology necessarily involves the calculation of snow and ice melt as a function of the surface energy balance. Numerical methods for simulating glacier melt are similar to

those for snowmelt but need to further take into account the significant albedo difference between snow and ice (Davaze et al., 2018; Fugazza et al., 2019; Naegeli et al., 2019). Simulating runoff from glaciers over timescales of years to decades requires the description of all components of the high-alpine water balance, the snow and ice melting processes, and the routing of runoff through the glacial and periglacial system. Semiempirical to process-based models have been proposed and applied with different spatial discretizations (e.g., Farinotti et al., 2012; Frans et al., 2018; Horton et al., 2006; Schaefler et al., 2007; Seibert et al., 2018). Glacio-hydrological studies over periods with strong glacier changes furthermore need to take into account the evolution of glacier area and ice thickness by physical ice-flow modeling or simplified approaches (e.g., Huss et al., 2010; Immerzeel et al., 2012).

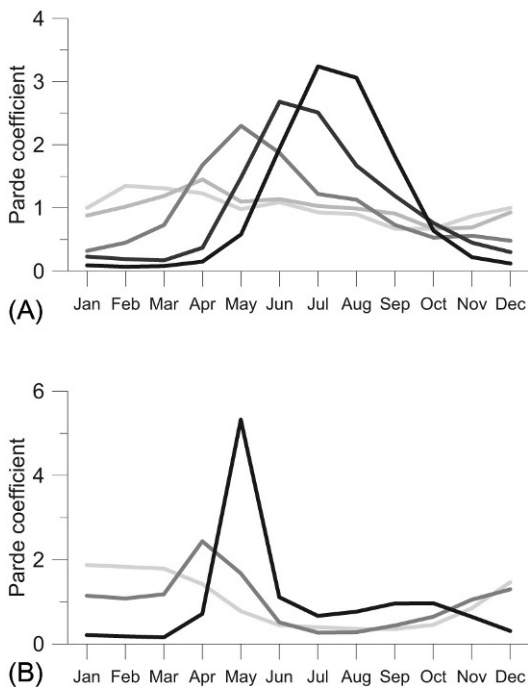
## 4.4 Hydrology of snow- and ice-covered catchments

### 4.4.1 Influence of snow on discharge

The most obvious feature of runoff in snow-dominated catchments is the large seasonality. Usually, there is a more or less pronounced spring flood, during which a large fraction of the annual runoff occurs for a few weeks. In highly glacierized catchments, the seasonality is even more pronounced with runoff basically following the available energy for melt. The runoff regime of catchments without snow influence often shows the opposite pattern, that is, low runoff during the summer due to energy being available for evaporation. In mountainous areas, the importance of snow and, thus, the seasonal differences increase with elevation and the annual maximum streamflow, is observed later for higher elevations (Fig. 4.11A; Weingartner and Aschwanden, 1992). In lowland catchments, a similar pattern can be observed when going from lower to higher latitudes (Fig. 4.11B). For larger river catchments, this means that the runoff from snow and glacial melt in upstream mountainous headwater catchments can play a more important role in relative terms during the summer months than on the annual average (Stahl et al., 2017; Viviroli and Weingartner, 2004). This can be illustrated by discharge along the River Rhine (Fig. 4.12): the runoff regime of the upper part is clearly dominated by snow and glacial melt, and the high summer runoff from this part of the catchment balances the low summer runoff contributions downstream.

During the late summer, glacial melt contributes far more than one might expect from the proportion of the area covered by glaciers. For the month of August, for instance, glacier storage change contributes on average about 7% of the streamflow in the River Rhine at the station Andernach, despite glaciers covering only 0.23% of the catchment area (Huss, 2011). The contributions of snowmelt are clearly larger than those of ice melt in the Rhine catchment. At Lobith (border Germany-Netherlands), ice melt contributes on average slightly more than 1%, whereas snowmelt is responsible for one-third of the discharge (Stahl et al., 2017). An analysis of discharge contributions over the past 100 years, however, showed that for a few extremely warm summers, when evaporation in the lower parts of the catchment was high, and glacial melt above the long-term average, the contribution of ice melt to discharge at Lobith increased for single days to almost 20%. Such high contributions were not reached for prolonged periods but the ice contribution was still more than 10% as a monthly average during such extreme periods (Stahl et al., 2017).

Another feature of runoff from snow-covered catchments, which is even more evident for glacierized catchments, as discussed later, is the observation of apparent diurnal variations in runoff with maximum values typically in the late afternoon (see Figs. 4.10 and 4.13).

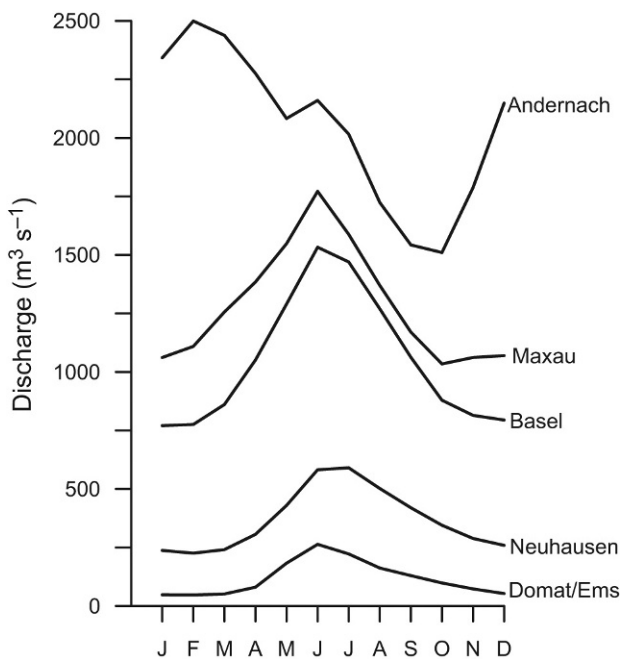
**FIG. 4.11**

Seasonal runoff variation in catchments with varying snow dominance. The Pardé coefficient is the long-term monthly mean runoff divided by the annual mean. The runoff regime varies with elevation (see (A) five catchments in Switzerland from low (*light gray*) to high (*black*) elevations: River Töss (mean elevation 650 m.a.s.l.), River Goldach (830 m), River Sense (1068 m), River Minster (1351 m), River Dischmabach (2372 m), and River Rhone at Gletsch (2719 m)) and latitude (see (B) three low-land catchments in Sweden from south to north: River Sege (*light gray*), River Fyris (*dark gray*), and River Vuoddasbäcken (*black*)).

*Panel (A): Data from Weingartner, R., Aschwanden, H., 1992. Abflussregimes als Grundlage zur Abschätzung von Mittelwerten des Abflusses. In: Federal Office for the Environment (Ed.), Hydrologischer Atlas der Schweiz. FOEN, Bern, Tafel 5.2. Panel (B): Data from SMHI, 1968–2012.*

Despite this seasonal variation with the highest runoff in spring (on average), in smaller catchments, peak flows are usually caused by rainfall, rather than snowmelt, since the latter is a comparatively slow process (Figs. 4.13 and 4.14). Only in larger catchments do the highest flow peaks originate from snowmelt, because melting simultaneously occurs over large areas.

Rain-on-snow events are of especial importance for flooding because next to rain input, the flood water is also formed by melted snow and, thus, the runoff coefficient of such an event may exceed one (Eriksson et al., 2013; Floyd and Weiler, 2008; Juras et al., 2017; Würzer and Jonas, 2018). In contrast to common snowmelt conditions, most of the energy causing the snowmelt during the rain-on-snow events comes from turbulent fluxes (sensible and latent heat), rather than radiative fluxes (Würzer et al., 2016). Energy balance calculations (mentioned already) show that the energy added to the snowpack through rainwater is small in comparison with the other energy fluxes on a daily or longer

**FIG. 4.12**

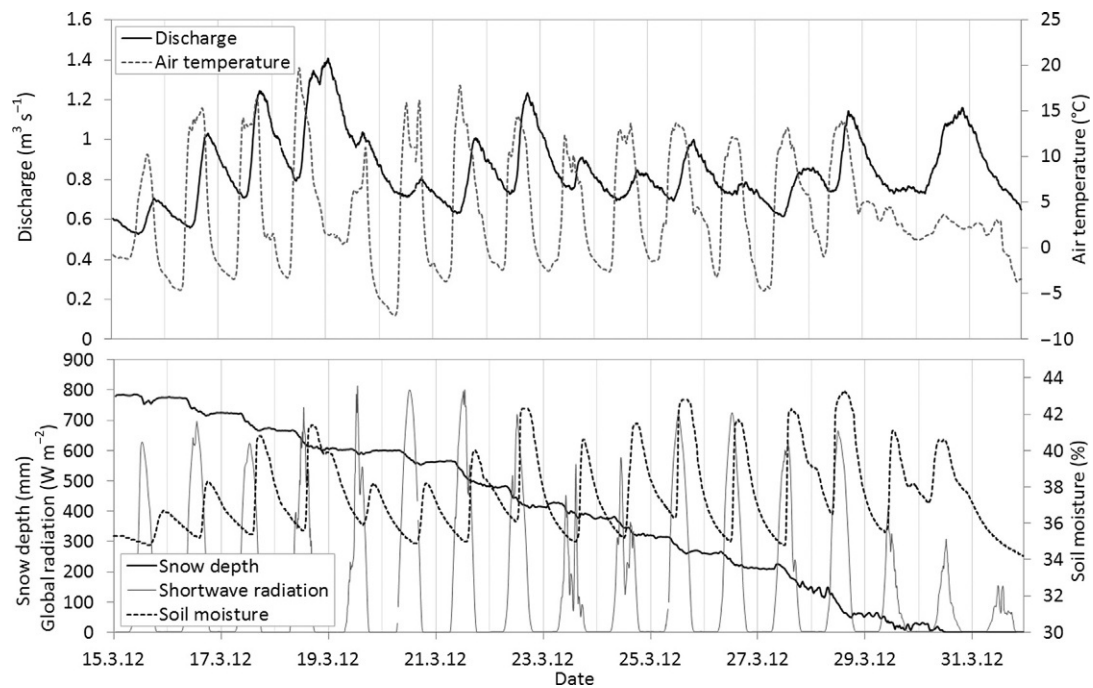
Seasonal runoff variation for different locations along the River Rhine.

*Data from Global Runoff Data Centre, GRDC.*

timescale. However, if rain falls on an already melting snowpack, the rainfall cannot be stored within the snowpack but quickly percolates downward ([Juras et al., 2017](#)). Many studies also show that the runoff response is highly variable, depending not only on meteorological conditions but also on physical properties of the snowpack (such as liquid water content or snow water equivalent), or characteristics of the rain event, such as the rain intensity and duration ([Rücker et al., 2019](#); [Wever et al., 2014](#); [Würzer and Jonas, 2018](#)). The interplay of all the mentioned factors controls the volume of the resulting runoff.

The processes mentioned earlier cause the quick response of the catchment to liquid precipitation ([Fig. 4.14](#)). Rain-on-snow floods are characterized by a steep rising limb of the hydrograph and high flood peaks in comparison with spring floods caused by snowmelt without additional liquid precipitation. The total flood volume depends on the volume of liquid precipitation and melting snow. However, catastrophic flood events are most often caused by a combination of several unfavorable circumstances: relatively high SWE both at higher and lower elevations, air temperatures significantly above the melting point at all elevations, high liquid precipitation, windy conditions causing turbulent heat exchange, ripe snowpack (isothermal conditions) and, before the rain-on-snow event, antecedent soil moisture, frozen soils, and existing river ice.

One of the biggest rain-on-snow events and resulting floods in Central Europe at the large scale occurred in the Danube River basin during the spring 2006. The flood mainly affected the area of

**FIG. 4.13**

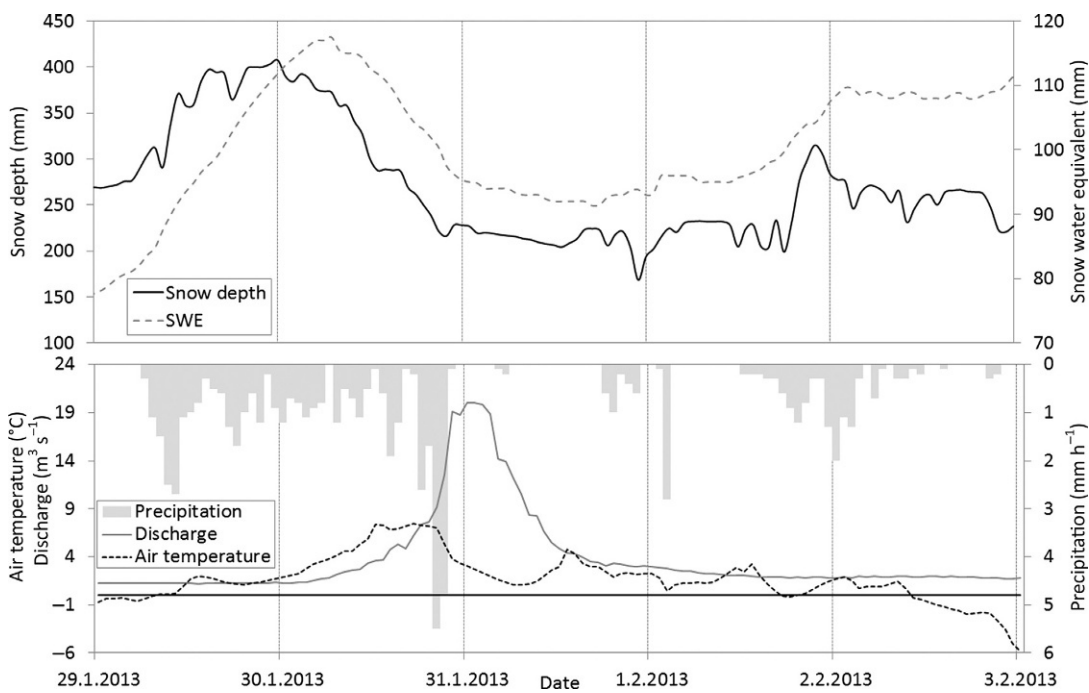
Snowmelt caused by high air temperature during the sunny weather in the Bystrice River basin, Krušné Mts., Czech Republic. Diurnal variation of the air temperature, snow depth, soil moisture, and discharge is typical for these kinds of situations. The soil was not frozen during this period. Typical diurnal variations of the snow depth are caused by freezing conditions during the nighttime which temporarily stops the snowmelt.

*Data from Charles University in Prague, Faculty of Science.*

the upper Danube River basin and some northern tributaries such as the Morava River, Váh River, and Tisza River. The main reasons for the flood were unusually high quantities of snow at medium elevations, together with high air temperature and liquid precipitation. Although the liquid precipitation was important but still not extreme at the large scale (it ranged from 50 mm to around 100 mm between 25 March and 13 April, depending on the sub-basin location), the high snow storage caused extreme flood peaks with return periods up to 100 years for some sub-basins, such as the Morava River and Danube River at Budapest (Wachter, 2007).

#### 4.4.2 Snowmelt runoff and climate change

Climate change has a significant impact on the hydrology of snow-covered catchments. For most of the Northern Hemisphere, changes in snowfall patterns are expected to emerge during the twenty-first century with some delay to the temperature signal. Although widespread negative snowfall trends are expected due to warming, positive trends may still occur over large areas of Eurasia and North America where temperatures remain sufficiently low and total precipitation increases (Krasting et al., 2013).

**FIG. 4.14**

Rain-on-snow event from Jan 29, 2013, to Feb 3, 2013, at the Modrava climate station, Šumava Mountains, Czech Republic. The different timing of peaks for the displayed variables (snow depth, SWE, air temperature, and discharge) can be seen to indicate the “sponge” effect of the snowpack with metamorphic changes of ice crystals and possible accumulation of liquid water in the snowpack (a decrease of snow depth with increasing SWE).

*Data from Charles University in Prague, Faculty of Science.*

Where snowfall declines, a transition is generally found from snowmelt runoff to rainfall runoff, with the exception of some basins in Central America, the Mediterranean, and Central Asia, where both snowmelt and rainfall runoff are projected to decrease (Mankin et al., 2015). The decline in snowfall also leads to shallower snowpack and thus an earlier end of the snowmelt seasons. This in turn is expected to effect a decrease in the water available for soil moisture recharge in spring and summer, as well as a drawdown of shallow groundwater (Huntington and Niswonger, 2012). As regards minimum flows after the end of the snowmelt period, studies in the Sierra Nevada Mountains have shown that annual minimum flow decreases by 9%–22% and occurs 3–7 days earlier for every 10% decline in the maximum of snow water equivalent (Godsey et al., 2014). Following from the shorter snow accumulation season and the earlier snowmelt peak, longer droughts are expected in widespread parts of snow-dominated regions (Wanders et al., 2015). Moreover, the amount of runoff formation in spring and summer decreases due to the reduced storage and thus less frequent exceedance of wetness thresholds that allow for effective runoff formation (Musselman et al., 2017). Conversely, more precipitation falling as rain in winter leads to an increased recharge of soil moisture during the accumulation season. The annual range and heterogeneity of water storage must thus be expected to increase (Wu et al., 2015).

Changes in snowmelt runoff are highly relevant for water resources: To date, snowmelt runoff fulfills human water demand that, with a shift to rainfall, would not be met at the right time during the year in almost 100 basins of the Northern Hemisphere, home to a total population of 1.9 billion people. Roughly one-third of these basins are potentially sensitive to changes in supply from snowmelt runoff, affecting a population of 1.45 billion. One-fifth of the basins face a considerable risk of both future decreases in snowmelt runoff and increases in demand not met by rainfall runoff, however with a lower total population of 27 Million (Mankin et al., 2015).

The occurrence of rain-on-snow events will probably also change in the future due to the increase in air temperature and precipitation during the winter (Beniston and Stoffel, 2016). Surfleet and Tullos (2013) assessed historical and predicted runoff data for the Santiam River basin in Oregon and concluded that the peak flows associated with rain-on-snow events will decrease at lower elevations while there will be a significant rise of the frequency of peak daily flows with a <5–10-year return period at medium to high altitudes. However, the overall frequency of rain-on-snow events was expected to decrease in the studied basin due to generally smaller amounts of snow. Simulations show a similar pattern for western North America in its entirety, with less frequent rain-on-snow events at lower elevations due to declining snowpack, but an overall increase of water available for runoff and thus a clearly increased flood risk at higher elevations (Musselman et al., 2018). For the Sitter River basin in the Swiss Pre-Alps, it was shown that the number of rain-on-snow events could increase up to 50% with a warming of 2°C–4°C, whereas a warming of more than 4°C would again lead to a decline (Beniston and Stoffel, 2016).

### 4.4.3 Influence of glaciers on discharge

Glaciers are an essential element of the hydrological cycle in alpine environments and are known to strongly influence the runoff regime of glacierized drainage basins at local to over-regional scales, even with only a minor degree of glacier coverage (Biemans et al., 2019; Hock, 2005; Immerzeel et al., 2019; Kaser et al., 2010). The significant influence of glaciers on the hydrological regime of mountainous catchments has been well documented in a number of studies (e.g., Barnett et al., 2005; Fountain and Tangborn, 1985; Kuhn and Batlogg, 1998; Meier and Tangborn, 1961; Vivenzio and Weingartner, 2004). Hock (2005) identified five specific characteristics of glacierized basins: (1) During years with glacier mass gain, specific runoff from the catchment is reduced while in years with mass loss, additional water from long-term glacial storage contributes to discharge; (2) The runoff regime in basins with a glacierization of more than a few percentage shows strong seasonal variations with small discharge over 6–8 months and peak runoff during the melting season; (3) Runoff is characterized by distinct diurnal variations with large amplitudes (Fig. 4.10); (4) Basins with an intermediate glacierization exhibit reduced interannual runoff fluctuations as melt and precipitation compensate for each other (Farinotti et al., 2012; Lang, 1986); and (5) Glacier runoff is positively correlated with air temperature, whereas it is negatively correlated with precipitation.

#### 4.4.3.1 Quantifying glacier contribution to runoff

Several studies have addressed the contribution of past, present, and future glacier melt to runoff (e.g., Huss, 2011; Jost et al., 2012; Kaser et al., 2010; Koboltschnig and Schöner, 2011; Pritchard, 2019; Weber et al., 2010). The percentage of glacial water in streamflow is considered a good proxy for future runoff changes related to the potential disintegration of glaciers with ongoing atmospheric warming. As

summarized by Radić and Hock (2014), a considerable disagreement exists in the literature about the definition of glacier contribution to runoff leading to major difficulties in comparing published estimates.

Among the six different concepts for quantifying glacier contribution detected by Radić and Hock (2014), two major groups can be separated: some studies consider only meltwater originating from the ablation area (i.e., bare-ice melt) as glacier runoff and explicitly exclude snowmelt over the glacier (e.g., Jost et al., 2012; Koboltschnig and Schöner, 2011; Racoviteanu et al., 2013; Stahl et al., 2008; Weber et al., 2010). Other papers define glacier contribution based on a water balance approach, thus taking into account all water derived from glacierized surfaces (Huss, 2011; Kaser et al., 2010; Lambrecht and Mayer, 2009; Neal et al., 2010). Evaluations of glacier contribution to runoff thus need to detail the applied approach in order to provide useful values for water resource management.

A straightforward and independent approach to determine the importance of snow and ice meltwater in streamflow runoff is the measurement of stable chemical isotopes that allow the direct quantification of the fractional contribution of the different runoff components in the analyzed sample (e.g., Collins, 1977; Finger et al., 2013; Racoviteanu et al., 2013; Taylor et al., 2001). This method is purely observational and does not require hydrological modeling or water-balance calculations for evaluating the meltwater contribution. An immediate comparison to the already mentioned approaches is, however, difficult as chemical analysis only refers to particle concentrations, whereas daily to seasonal runoff variations also propagate by differences in the hydraulic head, that is, through lakes. A reliable determination of glacier contribution by chemical analysis is thus only possible in the proglacial stream, but not in large-scale catchments.

#### 4.4.3.2 Glacier runoff and climate change

Strong changes in the storage and runoff characteristic of glacierized drainage basins are expected in response to climate change over the twenty-first century (Barnett et al., 2005; Braun et al., 2000; Hock et al., 2005; Huss et al., 2008; Stahl et al., 2008). Due to glacier recession, a significant decrease in glacier storage capacity is probable—glaciers store smaller amounts of water in winter and thus release less during the melting season (Fig. 4.8D). This reduction in the natural and beneficial capability of glaciers to smooth out runoff variability with their anti-cyclic behavior will be crucial in terms of water resource management (e.g., Chen and Ohmura, 1990; Schaeffli et al., 2019), as well as regarding the effects of extreme years such as the European heat wave of 2003 (Zappa and Kan, 2007). Far-reaching impacts due to glacier retreat in many of the earth’s mountain ranges are thus expected to be most severe in regions with summer-dry conditions (Brunner et al., 2019; Frans et al., 2018; Huss and Hock, 2018; Immerzeel et al., 2010; Kraaijenbrink et al., 2017; Lutz et al., 2014; Pritchard, 2019; Sorg et al., 2012; Van Tiel et al., 2018). The example of Finnelengletscher, Switzerland, shows that drainage basin runoff during the summer months might decrease by 50% or more due to a lack of snow and ice melt compared to the present situation (Fig. 4.8).

Huss and Hock (2018) assessed the impact of projected twenty-first-century climate change on the hydrological response of all glaciers around the globe using a detailed model constrained for each individual glacier worldwide. Regarding repercussions on future water management, two important aspects emerged: (1) *peak water*—a tipping point marking the transition, between an increase in annual glacier runoff due to higher melt rates and a decrease due to shrinking glacier area, is close in many large-scale basins. In catchments characterized by small glaciers, peak water has already been reached, whereas in regions with high glaciation and major ice volumes, it is expected to occur around 2050

**Table 4.4** Modeled future changes in glacier runoff for selected large-scale basins (data based on Huss and Hock, 2018).

Basin	Glacierization (%)	Peak water (year)	$\Delta Q_{gl,2000-2090}$ (%)	Continent
Indus	2.37	2045 ± 17	-20 ± 11	Asia
Tarim	2.34	2051 ± 13	-18 ± 13	Asia
Brahmaputra	3.21	2049 ± 18	-27 ± 9	Asia
Aral Sea Basin	1.23	2051 ± 14	-33 ± 12	Asia
Ganges	1.09	2044 ± 21	-21 ± 9	Asia
Yukon	1.15	2054 ± 19	+10 ± 12	North America
Fraser	1.04	2016 ± 14	-66 ± 9	North America
Yangtze	0.13	2028 ± 13	-35 ± 7	Asia
Columbia	0.28	2010 ± 14	-74 ± 9	North America
Colorado	0.41	2011 ± 10	-48 ± 15	South America
Jockulsarlon F.	15.03	2064 ± 22	+9 ± 15	Europe
Rhone	0.93	2006 ± 7	-61 ± 12	Europe
Danube	0.05	2006 ± 4	-74 ± 8	Europe
Rio Santa	1.67	2012 ± 25	+38 ± 34	South America

Glacierization refers to ice-covered fraction of the overall basin by around 2010 and is derived from glacier inventories. Peak water is the year with maximum annual runoff yield from glaciers, and  $\Delta Q_{gl,2000-2090}$  is the computed change in a runoff between the periods 1990–2010 and 2080–2100 originating from surfaces glacierized today. Results refer to a medium CO<sub>2</sub>-emission scenario (RCP4.5) and represent a mean of 14 global circulation models ± 1 standard deviation. The basins are ordered according to decreasing present-day glacier area.

(Table 4.4) and (2) glacier runoff during the summer months is subject to a substantial reduction until the end of the century across all mountain ranges globally (Table 4.4). The regional climate, in particular the seasonality of precipitation, is, however, crucial in determining whether these projected glacier runoff changes will significantly affect actual water availability. In basins with presently low glacier contribution to runoff during the melting season, glacier changes have limited (or only local) relevance to future water management (e.g., Ganges, Brahmaputra, and Danube). In regions with a summer-dry climate and considerable glacierization, however, present ice-melt contributions are often considerable, leading to major impacts on water availability towards the end of the twenty-first century (e.g., Indus, Tarim, and Aral Sea; Huss and Hock, 2018; Pritchard, 2019).

The recent decline of glacier ice volume observed in all regions around the globe (Zemp et al., 2019) is a major concern regarding sea-level rise (see also chapter by Allison et al., 2020). Until the end of the twenty-first century, melting glaciers are expected to raise global sea-level by 0.1–0.2 m (Hock et al., 2019). From a hydrological perspective it is, however, important to mention that for several reasons, not all glacial meltwater will immediately contribute to sea-level rise (Haeberli and Linsbauer, 2013): (1) In polar regions, glacier ice is partly grounded below sea level and is thus not a net contribution when removed. This factor accounts for a reduction in effective sea-level rise due to glacier wastage of about 10% at a global scale (Haeberli and Linsbauer, 2013; Huss and Hock, 2015); (2) In a deglaciating landscape, the formation of new proglacial lakes can be observed (Haeberli et al., 2016; Magnin et al., 2020). These lake basins store some of the glacial meltwater, but might also represent a severe

hazard potential (Clague and O'Connor, 2021; Haeberli et al., 2019; Haeberli and Whiteman, 2021). Natural or artificial lakes in a deglaciating landscape might also have a considerable potential related to hydropower production and seasonal water storage (Farinotti et al., 2019); (3) Some glacierized regions (mostly in High Mountain Asia) are drained to endorheic basins that have no direct connection to the ocean. Furthermore, glacial meltwater might also contribute to groundwater recharge (Lemieux et al., 2008; Vincent et al., 2019). Overall, these factors lead to a small but systematic decrease in the sea-level rise contribution from melting glacier ice and thus need to be accounted for.

#### 4.4.4 River ice

River ice (Fig. 4.15) is an important feature of many rivers, which can contribute to extreme events. The cooling of water during the fall and winter differs for flowing river water compared to lakes. While in lakes, after an initial cooling to about 4 °C, a thermal stratification develops with only the upper water layer cooling down further, usually the entire water column cools down at the same rate in rivers due to mixing of the flowing water. The cooling is mainly caused by the negative long-wave radiation budget, the convective heat transfer to the atmosphere, and the cooling effect of evaporation. Precipitation can have some cooling effect especially in the case of snow when energy is consumed for melting. Groundwater is commonly the main contribution to river flow and can be a significant source of energy due to the higher temperatures. When river water cools down to 0 °C, various types of ice can form (Prowse, 2005). These include border ice along the river shores and frazil ice. The latter is made up of loose ice crystals that start forming when the water is supercooled (<−0.05 °C) and both grow and aggregate into larger ice pieces. With continued cooling, eventually a complete ice cover can develop. This ice cover can break up depending on the factors such as ice thickness and strength, river geometry, flow velocity, and water levels. Frozen rivers are also important for local communities for traveling, and the



FIG. 4.15

Water, snow, and ice in the Roseg Valley, Samedan, Switzerland.

Photo: Jan Seibert.

declining periods with safe ice conditions due to climate warming can, thus, affect these communities (Brown et al., 2018).

In cold climates, ice breakup usually occurs as one major spring event. The importance of this type of event in cold climates is also indicated by many historical records, which have been used as climatological indicators especially for times before measurements started (Kajander, 1993; Magnuson et al., 2000; Rannie, 1983). In more temperate cold climates, there might be several freeze-breakup cycles during one winter season. Remote sensing, such as MODIS imagery, provides new possibilities to monitor the dynamics of frozen rivers (Cooley and Pavelsky, 2016). On the ground, time-lapse cameras together with automated image-processing algorithms allow for new observation methods of ice-covered rivers such as the portion of ice-covered areas and its temporal variation (Ansari et al., 2017). During the ice breakup, high water levels can be caused by ice dams and severe floodings might be due to failure of such ice dams (Prowse, 2005). Although river ice can cause high flows, the more surprising observation is that runoff in winter and spring can be affected by temporary water storage within rivers driven by hydraulic friction in situations with river ice (Prowse and Carter, 2002). Winter runoff thus decreases and spring runoff is enhanced.

#### 4.4.5 Seasonally frozen soil and permafrost

The freezing of soil, both permanently and seasonally, can have significant impacts on runoff generation processes (Hayashi, 2013). Soil freezing starts when the temperatures at the soil surface decrease below zero degrees, which causes a temperature gradient towards the surface from the so-called freezing front. The soil energy balance is highly dependent on the presence of a snow cover. Due to the low thermal conductivity of snow, the snow has an insulating effect and a snow cover of 20–30 cm is enough to inhibit further freezing from above (Hirota et al., 2006), whereas freezing from below in permafrost regions occurs independently of snow cover. In ice-rich frozen soils, conductive heat transfer is dominant because the ice prevents advective transfer by liquid water or vapor, which would otherwise be more important. The most considerable effect of soil frost on runoff generation is the changed infiltration capacity. Detailed modeling of soil frost and its effects on hydraulic conductivity is challenging, and approaches such as using two flow domains (slow and quick flow) have to be used to better predict water fluxes in frozen soils (Stähli et al., 1996, 1999). A general observation, however, is that the soil water content at the time of freezing largely influences the resulting infiltration capacity. In the case of wet soils at the beginning of freezing, the frozen soil can form an almost impermeable layer. This can generate a complex interaction between climate, snow, and runoff. For instance, in boreal catchments, higher runoff peaks might be observed after snow-poor winters compared to snow-rich winters, which might seem counterintuitive at first. The explanation is that during the winters with less snow there is less insulation and deeper frozen soil will develop, which in turn would lead to restricted infiltration and thus higher runoff peaks. Because snow depth and soil frost are usually inversely correlated, the presence of soil frost might seldom lead to extreme floods (Lindström et al., 2002). However, the interplay between snow accumulation and soil frost is complex and the conditions during early winter are most important (Bayard et al., 2005; Stähli et al., 2001). In many areas, especially within forests, soil frost does not usually entirely stop infiltration, but rates can be significantly reduced. In wetlands, on the contrary, soil frost can generate an impermeable layer and cause overland flow (Laudon et al., 2007). At larger scales, the effect of other factors often masks a clear relationship between snow accumulation, soil frost, and runoff (Shanley and Chalmers, 1999).

Permafrost can have even larger effects on hydrological processes. Permafrost is subsurface ground material (soil, sediment, bedrock, etc.) that has a temperature below 0°C for consecutive years and exists in about 20%–25% of the earth’s land surface, in polar and circumpolar regions, and in alpine areas at lower latitudes (Dankers, 2008). In areas with permafrost, the upper parts of the ground usually thaw and refreeze seasonally. This part of the ground is termed the “active layer,” begins to form during the spring snowmelt, and reaches its greatest depth in September. The seasonal changes and resulting thickness of the active layer are primary controls on the hydrologic response in catchments with permafrost (Shanley and Chalmers, 1999). During the summer, the active layer warms, increasing the ground portion available for infiltration and liquid water storage, which then again decreases during the winter. Ice-rich permafrost can decrease the hydraulic conductivity of the ground dramatically, so that an almost impermeable layer can be formed. In this case, groundwater (or saturated conditions) occur both seasonally in the active layer above the perennially frozen part of the ground and below this zone. With the impermeable layer, permafrost can result in increased soil moisture in the active layer and might even result in perched lakes. When water infiltrates into the deeper groundwater in areas with higher elevations, confined aquifers with artesian wells can be formed in neighboring areas of lower elevation (Hinzman et al., 2005).

#### 4.4.5.1 Permafrost and climate change

Large-scale changes in permafrost thaw can provide a key indicator of climate change (Box et al., 2019); however, direct observations of permafrost are primarily limited to local scales. A need exists for both more local studies on permafrost change in relation to streamflow dynamics and indirect methods that estimate effects on larger scales. At the catchment level, permafrost thaw affects hydrology as the active layer becomes deeper, hydrologic permeability increases due to ice loss, and the release of stored water may significantly affect streamflow dynamics. Changes in observed streamflow dynamics quantified by recession coefficients have been used to estimate permafrost thawing rates in northern Sweden (Lyon et al., 2009). This method was further extended to the Yukon river basin (Lyon and Destouni, 2010), a region covering large parts of Alaska and northern Canada with varying permafrost conditions. Changes in streamflow dynamics, quantified by changes in recession flow properties, were found to agree well with the observations of permafrost thawing. In addition, catchments with the largest increases in effective depth to permafrost (estimated by recession flow properties) were found to have the largest increases in relative observed groundwater flow, indicative of the amount of permafrost thawing. Other studies have shown changes in streamflow dynamics due to changes in permafrost thaw, including increased contribution of deeper groundwater flow (Bense et al., 2012; Frey and McClelland, 2009), increased groundwater contribution to baseflow (Jacques and Sauchyn, 2009; Kolosov et al., 2016; Walvoord and Striegl, 2007), changes in temporal runoff characteristics, including higher baseflow (Woo et al., 2008), and declining groundwater levels (Cheng and Jin, 2013; Jin et al., 2009). Furthermore, the hydrologic connectivity of a catchment may change, affecting the flow rates and amounts along different paths (Hinzman et al., 2005; Rogger et al., 2017). These changes may drive transitional permafrost environments from surface water-dominated to groundwater-dominated (Frey and McClelland, 2009). In addition to physical changes, impacts of permafrost thaw on geochemistry have also been observed. With a thickening of the active layer and melting of near-surface ground ice, changes in fluxes of inorganic chemicals have been observed. Increases of major ion delivery to surface freshwater have been reported in both polar and mountain areas (Colombo et al., 2018), a result

of a deepening of flow pathways and an increased contribution of deep, highly mineralized groundwater and enhanced interactions of soil water.

Increasing temperatures also cause permafrost degradation (a decrease in volume of a body of permafrost) and surface subsidence (Streltskiy, 2021). Climate change, together with increasing development, will result in a growing number of permafrost-related impacts in addition to hydrology, including on water quality, vegetation, livelihoods, infrastructure, and geohazards (e.g., an increased risk for slope failures in mountainous regions; Deline et al., 2021). An improved understanding of permafrost in poorly studied remote regions, including polar and high-elevation regions, and especially in extreme mountain environments, including the Himalayas, where permafrost areas are considerable (Deline et al., 2021), will help to anticipate and mitigate these impacts, and to understand the role and impact of permafrost on hydrology at different scales. New technologies, including InSAR (interferometric synthetic aperture radar) and altimetry observations of glacier and permafrost changes in remote regions, will help in providing improved information on the current evolution of permafrost change on larger scales, and to provide improved future scenarios (Jones et al., 2018).

---

## 4.5 Concluding remarks

In this chapter, we have discussed various aspects of snow and ice in the water cycle. In cold climates, the freezing–thawing threshold is crucial for many processes influencing the hydrology at different scales. Due to this temperature threshold, snow- and glacier-dominated catchments might react very sensitively to climate variations, especially for those parts of the year where temperatures today are around 0°C. In general, it is expected that higher temperatures will shorten the snow season and reduce glacier storage capacity leading to changes in seasonal runoff. Although the exact impacts on the length of the snow cover period will vary, one can estimate that with a mean temperature increase of 3°C, the snow cover period can be easily shortened by about a month. Besides direct impacts on the hydrology, this also has indirect impacts through possible changes in the vegetation, because the extension of the part of the year without snow cover implies a prolongation of the growing season. As discussed earlier, with a decreased snow cover in winter, higher temperatures might paradoxically lead to an increased cooling of soils due to the missing insulation of the snow. For permafrost areas, the deeper active layer might result in increased infiltration rates and storage and thus reduced overland flow. A good understanding of the role of snow and ice in the hydrology of cold region catchments is crucial for addressing natural hazards and water management in these sensitive systems both today and in the future. Due to the often difficult conditions, field observations are still limiting our knowledge of the hydrological processes in these regions and further studies combining field observations, remote sensing, and modeling are needed for an improved understanding.

---

## References

- Allison, I., Paul, F., Colgan, W., King, M., 2021. Ice sheets, glaciers and sea level. In: Haeberli, W., Whiteman, C. (Eds.), *Snow and Ice-Related Hazards, Risks and Disasters*. Elsevier, pp. 707–740.
- Anderton, S.P., White, S.M., Alvera, B., 2004. Evaluation of spatial variability in snow water equivalent for a high mountain catchment. *Hydrol. Process.* 18, 435–453. <https://doi.org/10.1002/hyp.1319>.

- Ansari, S., Rennie, C.D., Seidou, O., Malenchak, J., Zare, S.G., 2017. Automated monitoring of river ice processes using shore-based imagery. *Cold Reg. Sci. Technol.* 142, 1–16. <https://doi.org/10.1016/j.coldregions.2017.06.011>.
- Arenson, L., Colgan, W., Marshall, H.P., 2021. Physical, thermal and mechanical properties of snow, ice and permafrost. In: Haeberli, W., Whiteman, C. (Eds.), *Snow and Ice-Related Hazards, Risks and Disasters*. Elsevier, pp. 35–71.
- Barnett, T.P., Adam, J.C., Lettenmaier, D.P., 2005. Potential impacts of a warming climate on water availability in snow-dominated regions. *Nature* 438, 303–309. <https://doi.org/10.1038/nature04141>.
- Bavera, D., Bavay, M., Jonas, T., Lehning, M., De Michele, C., 2014. A comparison between two statistical and a physically-based model in snow water equivalent mapping. *Adv. Water Resour.* 63, 167–178. <https://doi.org/10.1016/j.advwatres.2013.11.011>.
- Bayard, D., Stähli, M., Pariaux, A., Flühler, H., 2005. The influence of seasonally frozen soil on the snowmelt runoff at two Alpine sites in southern Switzerland. *J. Hydrol.* 309, 66–84. <https://doi.org/10.1016/j.jhydrol.2004.11.012>.
- Beedle, M.J., Menounos, B., Wheate, R., 2014. An evaluation of mass-balance methods applied to Castle Creek Glacier, British Columbia, Canada. *J. Glaciol.* 60, 262–276. <https://doi.org/10.3189/2014JoG13J091>.
- Beniston, M., Stoffel, M., 2016. Rain-on-snow events, floods and climate change in the Alps: events may increase with warming up to 4 °C and decrease thereafter. *Sci. Total Environ.* 571, 228–236. <https://doi.org/10.1016/j.scitotenv.2016.07.146>.
- Bense, V.F., Kooi, H., Ferguson, G., Read, T., 2012. Permafrost degradation as a control on hydrogeological regime shifts in a warming climate. *J. Geophys. Res. Earth Surf.* 117, 1–18. <https://doi.org/10.1029/2011JF002143>.
- Bernhardt, M., Schulz, K., Liston, G.E., Zängl, G., 2012. The influence of lateral snow redistribution processes on snow melt and sublimation in alpine regions. *J. Hydrol.* 424–425, 196–206. <https://doi.org/10.1016/j.jhydrol.2012.01.001>.
- Berthier, E., Cabot, V., Vincent, C., Six, D., 2016. Decadal region-wide and glacier-wide mass balances derived from multi-temporal aster satellite digital elevation models. Validation over the mont-blanc area. *Front. Earth Sci.* 4, 1–16. <https://doi.org/10.3389/feart.2016.00063>.
- Beven, K.J., 2001. *Rainfall-Runoff Modelling: The Primer*. Wiley, Chichester.
- Biemans, H., Siderius, C., Lutz, A.F., Nepal, S., Ahmad, B., Hassan, T., von Bloh, W., Wijngaard, R.R., Wester, P., Shrestha, A.B., Immerzeel, W.W., 2019. Importance of snow and glacier meltwater for agriculture on the Indo-Gangetic Plain. *Nat. Sustain.* 2, 594–601. <https://doi.org/10.1038/s41893-019-0305-3>.
- Bolch, T., Sandberg Sørensen, L., Simonsen, S.B., Mölg, N., Machguth, H., Rastner, P., Paul, F., 2013. Mass loss of Greenland's glaciers and ice caps 2003–2008 revealed from ICESat laser altimetry data. *Geophys. Res. Lett.* 40, 875–881. <https://doi.org/10.1002/grl.50270>.
- Bormann, K.J., Brown, R.D., Derksen, C., Painter, T.H., 2018. Estimating snow-cover trends from space. *Nat. Clim. Chang.* 8, 924–928. <https://doi.org/10.1038/s41558-018-0318-3>.
- Box, J.E., Colgan, W.T., Christensen, T.R., Schmidt, N.M., Lund, M., Parmentier, F.J.W., Brown, R., Bhatt, U.S., Euskirchen, E.S., Romanovsky, V.E., Walsh, J.E., Overland, J.E., Wang, M., Corell, R.W., Meier, W.N., Wouters, B., Mernild, S., Mård, J., Pawlak, J., Olsen, M.S., 2019. Key indicators of Arctic climate change: 1971–2017. *Environ. Res. Lett.* 14. <https://doi.org/10.1088/1748-9326/aafcb>.
- Braithwaite, R.J., Olesen, O.B., 1989. Calculation of glacier ablation from air-temperature, west Greenland. In: Oerlemans, J. (Ed.), *Glacier Fluctuations and Climatic Change, Glaciology and Quaternary Geology*. Kluwer Academic Publishers, Dordrecht, pp. 219–233.
- Braun, L.N., Weber, M., Schulz, M., 2000. Consequences of climate change for runoff from Alpine regions. *Ann. Glaciol.* 31, 19–25.
- Brown, D.R.N., Brinkman, T.J., Verbyla, D.L., Brown, C.L., Cold, H.S., Hollingsworth, T.N., 2018. Changing river ice seasonality and impacts on interior Alaskan communities. *Weather. Clim. Soc.* 10, 625–640. <https://doi.org/10.1175/WCAS-D-17-0101.1>.

- Brown, R.D., Goodison, B.E., 2005. Snow cover. In: Anderson, M.G. (Ed.), *Encyclopedia of Hydrological Sciences*. John Wiley and Sons, Chichester, UK, pp. 1–12.
- Brun, F., Berthier, E., Wagnon, P., Kääb, A., Treichler, D., 2017. A spatially resolved estimate of High Mountain Asia glacier mass balances from 2000 to 2016. *Nat. Geosci.* 10, 668–673. <https://doi.org/10.1038/ngeo2999>.
- Brunner, M.I., Farinotti, D., Zekollari, H., Huss, M., Zappa, M., 2019. Future shifts in extreme flow regimes in Alpine regions. *Hydrol. Earth Syst. Sci. Discuss.*, 1–26. <https://doi.org/10.5194/hess-2019-144>.
- Bühler, Y., Marty, M., Egli, L., Veitinger, J., Jonas, T., Thee, P., Ginzler, C., 2015. Snow depth mapping in high-alpine catchments using digital photogrammetry. *Cryosphere* 9, 229–243. <https://doi.org/10.5194/tc-9-229-2015>.
- Bühler, Y., Adams, M.S., Bösch, R., Stoffel, A., 2016. Mapping snow depth in alpine terrain with unmanned aerial systems (UASs): potential and limitations. *Cryosphere* 10, 1075–1088. <https://doi.org/10.5194/tc-10-1075-2016>.
- Chen, J., Ohmura, A., 1990. Estimation of Alpine glacier water resources and their change since the 1870s. In: *Hydrology in Mountainous Regions. I—Hydrological Measurements; the Water Cycle (Proceedings of Two Lausanne Symposia, August 1990)*. IAHS Publ. No. 193, pp. 127–136.
- Cheng, G., Jin, H., 2013. Permafrost and groundwater on the Qinghai-Tibet Plateau and in northeast China. *Hydrogeol. J.* 21, 5–23. <https://doi.org/10.1007/s10040-012-0927-2>.
- Clague, J.J., O'Connor, J.E., 2021. Glacier-related outburst floods. In: Haeberli, W., Whiteman, C. (Eds.), *Snow and Ice-Related Hazards, Risks and Disasters*. Elsevier, pp. 467–499.
- Cogley, J.G., Hock, R., Rasmussen, L.A., Arendt, A.A., Bauder, A., Braithwaite, R.J., Jansson, P., Kaser, G., Möller, M., Nicholson, L., Zemp, M., 2011. Glossary of Glacier Mass Balance and Related Terms, IHP-VII Technical Documents in Hydrology No. 86, IACS Contribution No. 2. UNESCO-IHP, Paris.
- Collins, D.N., 1977. Hydrology of an Alpine glacier as indicated by the chemical composition of meltwater. *Z. Gletscherk. Glazialgeol.* 13, 219–238.
- Colombo, N., Salerno, F., Gruber, S., Freppaz, M., Williams, M., Fratianni, S., Giardino, M., 2018. Review: impacts of permafrost degradation on inorganic chemistry of surface fresh water. *Global Planet. Change* 162, 69–83. <https://doi.org/10.1016/j.gloplacha.2017.11.017>.
- Cooley, S.W., Pavelsky, T.M., 2016. Spatial and temporal patterns in Arctic river ice breakup revealed by automated ice detection from MODIS imagery. *Remote Sens. Environ.* 175, 310–322. <https://doi.org/10.1016/j.rse.2016.01.004>.
- Dankers, R., Bierkens, M.F.P., 2008. Arctic and snow hydrology. In: Dolman, A.J., Troch, P.A. (Eds.), *Climate and the Hydrological Cycle*. International Association of Hydrological Sciences, pp. 137–156.
- Davaze, L., Rabatel, A., Arnaud, Y., Sirguey, P., Six, D., Letreguilly, A., Dumont, M., 2018. Monitoring glacier albedo as a proxy to derive summer and annual surface mass balances from optical remote-sensing data. *Cryosphere* 12, 271–286. <https://doi.org/10.5194/tc-12-271-2018>.
- Davison, B., Pietroniro, A., 2005. Hydrology of snowcovered basins. In: Anderson, M.G. (Ed.), *Encyclopedia of Hydrological Sciences*. John Wiley and Sons, Chichester, UK, pp. 1–19.
- De Fleurian, B., Werder, M.A., Beyer, S., Brinkerhoff, D.J., Delaney, I., Dow, C.F., Downs, J., Gagliardini, O., Hoffman, M.J., Hooke, R.L., Seguinot, J., Sommers, A.N., 2018. SHMIP the subglacial hydrology model inter-comparison Project. *J. Glaciol.* 64, 897–916. <https://doi.org/10.1017/jog.2018.78>.
- De Michele, C., Avanzi, F., Passoni, D., Barzaghi, R., Pinto, L., Dosso, P., Ghezzi, A., Gianatti, R., Della Vedova, G., 2016. Using a fixed-wing UAS to map snow depth distribution: an evaluation at peak accumulation. *Cryosphere* 10, 511–522. <https://doi.org/10.5194/tc-10-511-2016>.
- Deline, P., Gruber, S., Aman, F., Bodin, X., Delaloye, R., Faillettaz, J., Fischer, L., Geertsema, M., Giardino, M., Hasler, A., Kirkbride, M., Krautblatter, M., Magnin, F., McColl, S., Ravanel, L., Schoeneich, P., Weber, S., 2021. Ice loss from glaciers and permafrost and related slope instability in high-mountain regions. In: Haeberli, W., Whiteman, C. (Eds.), *Snow and Ice-Related Hazards, Risks and Disasters*. Elsevier, pp. 501–540.

- DeWalle, D.R., Rango, A., 2008. *Principles of Snow Hydrology*. Cambridge University Press, Cambridge.
- Dingman, S.L., 2008. *Physical Hydrology*, second ed. Waveland Press Inc.
- Dong, C., 2018. Remote sensing, hydrological modeling and in situ observations in snow cover research: a review. *J. Hydrol.* 561, 573–583. <https://doi.org/10.1016/j.jhydrol.2018.04.027>.
- Dozier, J., Bair, E.H., Davis, R.E., 2016. Estimating the spatial distribution of snow water equivalent in the world's mountains. *Wiley Interdiscip. Rev. Water* 3, 461–474. <https://doi.org/10.1002/wat2.1140>.
- Dussaillant, I., Berthier, E., Brun, F., Masiokas, M., Hugonet, R., Favier, V., Rabatel, A., Pitte, P., Ruiz, L., 2019. Two decades of glacier mass loss along the Andes. *Nat. Geosci.* 12, 802–808. <https://doi.org/10.1038/s41561-019-0432-5>.
- Eckerstorfer, M., Christiansen, H.H., 2012. Meteorology, topography and snowpack conditions causing two extreme mid-winter slush and wet slab avalanche periods in High Arctic Maritime Svalbard. *Permafro. Periglac. Process.* 23, 15–25. <https://doi.org/10.1002/ppp.734>.
- Eckerstorfer, M., Bühler, Y., Frauenfelder, R., Malnes, E., 2016. Remote sensing of snow avalanches: recent advances, potential, and limitations. *Cold Reg. Sci. Technol.* 121, 126–140. <https://doi.org/10.1016/j.coldregions.2015.11.001>.
- Egli, L., Jonas, T., Meister, R., 2009. Comparison of different automatic methods for estimating snow water equivalent. *Cold Reg. Sci. Technol.* 57, 107–115. <https://doi.org/10.1016/j.coldregions.2009.02.008>.
- Egli, L., Jonas, T., Grünwald, T., Schirmer, M., Burlando, P., 2012. Dynamics of snow ablation in a small Alpine catchment observed by repeated terrestrial laser scans. *Hydrol. Process.* 26, 1574–1585. <https://doi.org/10.1002/hyp.8244>.
- Eriksson, D., Whitson, M., Luce, C.H., Marshall, H.P., Bradford, J., Benner, S.G., Black, T., Hetrick, H., McNamara, J.P., 2013. An evaluation of the hydrologic relevance of lateral flow in snow at hillslope and catchment scales. *Hydrol. Process.* 27, 640–654. <https://doi.org/10.1002/hyp.9666>.
- Essery, R., 2003. Aggregated and distributed modelling of snow cover for a high-latitude basin. *Global Planet. Change* 38, 115–120. [https://doi.org/10.1016/S0921-8181\(03\)00013-4](https://doi.org/10.1016/S0921-8181(03)00013-4).
- Farinotti, D., Magnusson, J., Huss, M., Bauder, A., 2010. Snow accumulation distribution inferred from time-lapse photography and simple modelling. *Hydrol. Process.* 24, 2087–2097. <https://doi.org/10.1002/hyp.7629>.
- Farinotti, D., Usselmann, S., Huss, M., Bauder, A., Funk, M., 2012. Runoff evolution in the Swiss Alps: projections for selected high-alpine catchments based on ENSEMBLES scenarios. *Hydrol. Process.* 26, 1909–1924. <https://doi.org/10.1002/hyp.8276>.
- Farinotti, D., Round, V., Huss, M., Compagno, L., Zekollari, H., 2019. Large hydropower and water-storage potential in future glacier-free basins. *Nature* 575, 341–344. <https://doi.org/10.1038/s41586-019-1740-z>.
- Federer, C.A., Pierce, R.S., Hornbeck, J.W., 1972. Snow management seems unlikely in the Northeast. In: *Proceedings Symposium on Watersheds in Transition*. American Water Resources Association, pp. 212–219.
- Fierz, C., Armstrong, R.L., Durand, Y., Etchevers, P., Greene, E., McClung, D.M., Nishimura, K., Satyawali, P.K., Sokratov, S.A., 2009. The international classification for seasonal snow on the ground. In: *IHP-VII Technical Documents in Hydrology No. 83, IACS Contribution No. 1. UNESCO-IHP*, Paris.
- Finger, D., Hugentobler, A., Huss, M., Voinesco, A., Wernli, H., Fischer, D., Weber, E., Jeannin, P.-Y., Kauzlaric, M., Wirz, A., Vennemann, T., Hüslar, F., Schädler, B., Weingartner, R., 2013. Identification of glacial meltwater runoff in a karstic environment and its implication for present and future water availability. *Hydrol. Earth Syst. Sci.* 17, 3261–3277. <https://doi.org/10.5194/hess-17-3261-2013>.
- Finsterwalder, S., Schunk, H., 1887. Der Suldenferner. *Zeitschrift des Dtsch. und Österreichischen Alpenvereins* 18, 72–89.
- Flowers, G.E., 2002. A multicomponent coupled model of glacier hydrology 1. Theory and synthetic examples. *J. Geophys. Res.* 107, 2287. <https://doi.org/10.1029/2001JB001122>.
- Floyd, W., Weiler, M., 2008. Measuring snow accumulation and ablation dynamics during rain-on-snow events: innovative measurement techniques. *Hydrol. Process.* 22, 4805–4812. <https://doi.org/10.1002/hyp.7142>.

- Fountain, A.G., Tangborn, W.V., 1985. The Effect of Glaciers on Streamflow Variations. *Water Resour. Res.* 21, 579–586.
- Fountain, A.G., Walder, S., 1998. Water flow through temperate glaciers. *Rev. Geophys.* 36, 299–328.
- Frans, C., Istanbulluoglu, E., Lettenmaier, D.P., Fountain, A.G., Riedel, J., 2018. Glacier recession and the response of summer streamflow in the Pacific Northwest United States, 1960–2099. *Water Resour. Res.* 54, 6202–6225. <https://doi.org/10.1029/2017WR021764>.
- Freudiger, D., Kohn, I., Seibert, J., Stahl, K., Weiler, M., 2017. Snow redistribution for the hydrological modeling of alpine catchments. *Wiley Interdiscip. Rev. Water* 4, e1232. 1–16 <https://doi.org/10.1002/wat2.1232>.
- Frey, K.E., McClelland, J.W., 2009. Impacts of permafrost degradation on arctic river biogeochemistry. *Hydrol. Process.* 23, 169–182. <https://doi.org/10.1002/hyp.7196>.
- Fugazza, D., Senese, A., Azzoni, R.S., Maugeri, M., Maragno, D., Diolaiuti, G.A., 2019. New evidence of glacier darkening in the Ortles-Cevedale group from Landsat observations. *Global Planet. Change* 178, 35–45. <https://doi.org/10.1016/j.gloplacha.2019.04.014>.
- Gardner, A.S., Moholdt, G., Cogley, J.G., Wouters, B., Arendt, A.A., Wahr, J., Berthier, E., Hock, R., Pfeffer, W.T., Kaser, G., Ligtenberg, S.R.M., Bolch, T., Sharp, M.J., Hagen, J.O., van den Broeke, M.R., Paul, F., 2013. A reconciled estimate of glacier contributions to sea level rise: 2003 to 2009. *Science* 340, 852–857. <https://doi.org/10.1126/science.1234532>.
- Garvelmann, J., Pohl, S., Weiler, M., 2013. From observation to the quantification of snow processes with a time-lapse camera network. *Hydrol. Earth Syst. Sci.* 17, 1415–1429. <https://doi.org/10.5194/hess-17-1415-2013>.
- Godsey, S.E., Kirchner, J.W., Tague, C.L., 2014. Effects of changes in winter snowpacks on summer low flows: case studies in the Sierra Nevada, California, USA. *Hydrol. Process.* 28, 5048–5064. <https://doi.org/10.1002/hyp.9943>.
- Grünewald, T., Schirmer, M., Mott, R., Lehning, M., 2010. Spatial and temporal variability of snow depth and ablation rates in a small mountain catchment. *Cryosphere* 4, 215–225. <https://doi.org/10.5194/tc-4-215-2010>.
- Haeberli, W., Linsbauer, A., 2013. Global glacier volumes and sea level—small but systematic effects of ice below the surface of the ocean and of new local lakes on land. *Cryosphere* 7, 817–821. <https://doi.org/10.5194/tc-7-817-2013>.
- Haeberli, W., Oerlemans, J., Zemp, M., 2019. The Future of Alpine Glaciers and Beyond. Oxford Research Encyclopedia of Climate Science, <https://doi.org/10.1093/acrefore/9780190228620.013.769>.
- Haeberli, W., Linsbauer, A., Cochachin, A., Salazar, C., Fischer, U.H., 2016. On the morphological characteristics of overdeepenings in high-mountain glacier beds. *Earth Surf. Process. Landf.* 41, 1980–1990. <https://doi.org/10.1002/esp.3966>.
- Haeberli, W., Whiteman, C., 2021. Snow and ice-related hazards, risks and disasters: facing challenges of rapid change and long-term commitments. In: Haeberli, W., Whiteman, C. (Eds.), *Snow and Ice-Related Hazards, Risks and Disasters*. Elsevier, pp. 1–34.
- Hayashi, M., 2013. The cold vadose zone: hydrological and ecological significance of frozen-soil processes. *Vadose Zo. J.* 12 (4), 1–8. <https://doi.org/10.2136/vzj2013.03.0064>.
- Helffricht, K., Hartl, L., Koch, R., Marty, C., Olefs, M., 2018. Obtaining sub-daily new snow density from automated measurements in high mountain regions. *Hydrol. Earth Syst. Sci.* 22, 2655–2668. <https://doi.org/10.5194/hess-22-2655-2018>.
- Hendriks, M.R., 2010. *Introduction to Physical Hydrology*. Oxford University Press.
- Hewitt, I.J., Schoof, C., Werder, M.A., 2012. Flotation and free surface flow in a model for subglacial drainage. Part 2. Channel flow. *J. Fluid Mech.* 702, 157–187. <https://doi.org/10.1017/jfm.2012.166>.
- Hinzman, L.D., Kane, D.L., Woo, M., 2005. Permafrost hydrology. In: Anderson, M.G. (Ed.), *Encyclopedia of Hydrological Sciences*. John Wiley and Sons, Chichester, UK, pp. 1–15.
- Hirota, T., Iwata, Y., Hayashi, M., Suzuki, S., Hamasaki, T., Sameshima, R., Takayabu, I., 2006. Decreasing soil-frost depth and its relation to climate change in Tokachi, Hokkaido, Japan. *J. Meteorol. Soc. Jpn.* 84, 821–833. <https://doi.org/10.2151/jmsj.84.821>.

- Hock, R., 1999. A distributed temperature-index ice- and snowmelt model including potential direct solar radiation. *J. Glaciol.* 45, 101–111.
- Hock, R., 2003. Temperature index melt modelling in mountain areas. *J. Hydrol.* 282, 104–115. [https://doi.org/10.1016/S0022-1694\(03\)00257-9](https://doi.org/10.1016/S0022-1694(03)00257-9).
- Hock, R., 2005. Glacier melt: a review of processes and their modelling. *Prog. Phys. Geogr.* 29, 362–391. <https://doi.org/10.1191/0309133305pp453ra>.
- Hock, R., Hooke, R.L., 1993. Evolution of the internal drainage system in the lower part of the ablation area of Storglaciären, Sweden. *Geol. Soc. Am. Bull.* 105, 537–546. [https://doi.org/10.1130/0016-7606\(1993\)105<0537:EOTIDS>2.3.CO;2](https://doi.org/10.1130/0016-7606(1993)105<0537:EOTIDS>2.3.CO;2).
- Hock, R., Jansson, P., 2005. Modeling glacier hydrology. In: Anderson, M.G. (Ed.), *Encyclopedia of Hydrological Sciences*. John Wiley and Sons, Chichester, UK, pp. 1–9.
- Hock, R., Noetzli, C., 1997. Areal melt and discharge modelling of Storglaciären, Sweden. *Ann. Glaciol.* 24, 211–216.
- Hock, R., Jansson, P., Braun, L.N., 2005. Modelling the response of mountain glacier discharge to climate warming. In: Huber, U.M., Bugmann, H.K.M., Reasoner, M.A. (Eds.), *Global Change and Mountain Regions. Advances in Global Change Research*. vol. 23. Springer, Dordrecht, pp. 243–252, [https://doi.org/10.1007/1-4020-3508-X\\_25](https://doi.org/10.1007/1-4020-3508-X_25).
- Hock, R., Rasul, G., Adler, C., Cáceres, B., Gruber, S., Hirabayashi, Y., Jackson, M., Kääb, A., Kang, S., Kutuzov, S., Milner, A., Molau, U., Morin, S., Orlove, B., Steltzer, H., Allen, S., Arenson, L., Baneerjee, S., Barr, I., Bórquez, R., Brown, L., Cao, B., Carey, M., Cogley, G., Fischlin, A., de Sherbinin, A., Eckert, N., Geertsema, M., Hagenstad, M., Honsberg, M., Hood, E., Huss, M., Jimenez Zamora, E., Kotlarski, S., Lefevre, P.-M., López Moreno, J.I., Lundquist, J., McDowell, G., Mills, S., Mou, C., Nepal, S., Noetzli, J., Palazzi, E., Pepin, N., Rixen, C., Shahgedanova, M., Skiles, S.M., Vincent, C., Vivioli, D., Weyhenmeyer, G., Sherpa, P.Y., Weyen, N., Wouters, B., Yasunari, T.J., You, Q., Zhang, Y., 2019. High mountain areas. In: Pörtner, H.-O., Roberts, D.C., Masson-Delmotte, V., Zhai, P., Tignor, M., Poloczanska, E., Weyen, N. (Eds.), *The Ocean and Cryosphere in a Changing Climate. Intergovernmental Panel on Climate Change*, pp. 2–90.
- Holko, L., Škvarenina, J., Kostka, Z., Frič, M., Staroň, J., 2009. Impact of spruce forest on rainfall interception and seasonal snow cover evolution in the Western Tatras Mountains, Slovakia. *Biologia (Bratisl.)* 64, 594–599. <https://doi.org/10.2478/s11756-009-0087-6>.
- Hood, J.L., Hayashi, M., 2010. Assessing the application of a laser rangefinder for determining snow depth in inaccessible alpine terrain. *Hydrol. Earth Syst. Sci.* 14, 901–910. <https://doi.org/10.5194/hess-14-901-2010>.
- Horton, P., Schaeffli, B., Mezghani, A., Hingray, B., Musy, A., 2006. Assessment of climate-change impacts on alpine discharge regimes with climate model uncertainty. *Hydrol. Process.* 20, 2091–2109. <https://doi.org/10.1002/hyp.6197>.
- Huntington, J.L., Niswonger, R.G., 2012. Role of surface-water and groundwater interactions on projected summertime streamflow in snow dominated regions: an integrated modeling approach. *Water Resour. Res.* 48, 1–20. <https://doi.org/10.1029/2012WR012319>.
- Huss, M., 2011. Present and future contribution of glacier storage change to runoff from macroscale drainage basins in Europe. *Water Resour. Res.* 47, 1–14. <https://doi.org/10.1029/2010WR010299>.
- Huss, M., Hock, R., 2015. A new model for global glacier change and sea-level rise. *Front. Earth Sci.* 3, 1–22. <https://doi.org/10.3389/feart.2015.00054>.
- Huss, M., Hock, R., 2018. Global-scale hydrological response to future glacier mass loss. *Nat. Clim. Chang.* 8, 135–140. <https://doi.org/10.1038/s41558-017-0049-x>.
- Huss, M., Farinotti, D., Bauder, A., Funk, M., 2008. Modelling runoff from highly glacierized alpine drainage basins in a changing climate. *Hydrol. Process.* 22, 3888–3902. <https://doi.org/10.1002/hyp>.
- Huss, M., Jouvet, G., Farinotti, D., Bauder, A., 2010. Future high-mountain hydrology: a new parameterization of glacier retreat. *Hydrol. Earth Syst. Sci.* 14, 815–829. <https://doi.org/10.5194/hess-14-815-2010>.
- Huss, M., Zemp, M., Joerg, P.C., Salzmann, N., 2014. High uncertainty in 21st century runoff projections from glacierized basins. *J. Hydrol.* 510, 35–48.

- Iken, A., Bindschadler, R.A., 1986. Combined measurements of subglacial water pressure and surface velocity of Findelengletscher, Switzerland: conclusions about drainage system and sliding mechanism. *J. Glaciol.* 32, 101–119.
- Immerzeel, W.W., van Beek, L.P.H., Bierkens, M.F.P., 2010. Climate change will affect the Asian water towers. *Science* 328, 1382–1385. <https://doi.org/10.1126/science.1183188>.
- Immerzeel, W.W., Shrestha, A.B., Bierkens, M.F.P., Beek, L.P.H., Konz, M., 2012. Hydrological response to climate change in a glacierized catchment in the Himalayas. *Clim. Chang.* 110, 721–736. <https://doi.org/10.1007/s10584-011-0143-4>.
- Immerzeel, W.W., Lutz, A.F., Andrade, M., Bahl, A., Biemans, H., Bolch, T., Hyde, S., Brumby, S., Davies, B.J., Elmore, A.C., Emmer, A., Feng, M., Fernández, A., Haritashya, U., Kargel, J.S., Koppes, M., Kraaijenbrink, P. D.A., Kulkarni, A.V., Mayewski, P., Nepal, S., Pacheco, P., Painter, T.H., Pellicciotti, F., Rajaram, H., Rupper, S., Sinisalo, A., Shrestha, A.B., Viviroli, D., Wada, Y., Xiao, C., Yao, T., Baillie, J.E.M., 2019. Importance and vulnerability of the world's water towers. *Nature*. <https://doi.org/10.1038/s41586-019-1822-y>.
- Irarrazaval, I., Werder, M.A., Linde, N., Irving, J., Herman, F., Mariethoz, G., 2019. Bayesian inference of subglacial channel structures from water pressure and tracer-transit time data: a numerical study based on a 2-D geostatistical modeling approach. *J. Geophys. Res. Earth Surf.* 124, 1625–1644. <https://doi.org/10.1029/2018JF004921>.
- Jacques, J.M.S., Sauchyn, D.J., 2009. Increasing winter baseflow and mean annual streamflow from possible permafrost thawing in the Northwest Territories, Canada. *Geophys. Res. Lett.* 36, 1–6. <https://doi.org/10.1029/2008GL035822>.
- Jagt, B., Lucieer, A., Wallace, L., Turner, D., Durand, M., 2015. Snow depth retrieval with UAS Using photogrammetric techniques. *Geosciences* 5, 264–285. <https://doi.org/10.3390/geosciences5030264>.
- Jansson, P., Hock, R., Schneider, T., 2003. The concept of glacier storage: a review. *J. Hydrol.* 282, 116–129. [https://doi.org/10.1016/S0022-1694\(03\)00258-0](https://doi.org/10.1016/S0022-1694(03)00258-0).
- Jenicek, M., Pevna, H., Matejka, O., 2018. Canopy structure and topography effects on snow distribution at a catchment scale: application of multivariate approaches. *J. Hydrol. Hydromechanics* 66, 43–54. <https://doi.org/10.1515/johh-2017-0027>.
- Jin, H., He, R., Cheng, G., Wu, Q., Wang, S., Lü, L., Chang, X., 2009. Changes in frozen ground in the source area of the yellow river on the qinghai-tibet plateau, China, and their eco-environmental impacts. *Environ. Res. Lett.* 4. <https://doi.org/10.1088/1748-9326/4/4/045206>.
- Jonas, T., Marty, C., Magnusson, J., 2009. Estimating the snow water equivalent from snow depth measurements in the Swiss Alps. *J. Hydrol.* 378, 161–167. <https://doi.org/10.1016/j.jhydrol.2009.09.021>.
- Jones, B.M., Bull, D.L., Farquharson, L.M., Baughman, C.A., Arp, C.D., Grosse, G., Günther, F., Kanevskiy, M., Iwahana, G., Bondurant, A.C., Buzard, R.M., Sachs, T., Nitze, I., Kasper, J.L., Frederick, J.M., Thomas, M., Mota, A., Jones, C., Roberts, J., Dallimore, S., Tweedie, C., Maio, C., Mann, D.H., Richmond, B., Gibbs, A., Xiao, M., Romanovsky, V.E., 2018. High temporal and spatial resolution satellite image observations for the past decade highlight complexities associated with permafrost coastal bluff erosion in the Arctic. In: 15th International Circumpolar Remote Sensing Symposium.
- Jost, G., Dan Moore, R., Weiler, M., Gluns, D.R., Alila, Y., 2009. Use of distributed snow measurements to test and improve a snowmelt model for predicting the effect of forest clear-cutting. *J. Hydrol.* 376, 94–106. <https://doi.org/10.1016/j.jhydrol.2009.07.017>.
- Jost, G., Moore, R.D., Menounos, B., Wheate, R., 2012. Quantifying the contribution of glacier runoff to streamflow in the upper Columbia River Basin, Canada. *Hydrol. Earth Syst. Sci.* 16, 849–860. <https://doi.org/10.5194/hess-16-849-2012>.
- Juras, R., Würzer, S., Pavlásek, J., Vitvar, T., Jonas, T., 2017. Rainwater propagation through snowpack during rain-on-snow sprinkling experiments under different snow conditions. *Hydrol. Earth Syst. Sci.* 21, 4973–4987. <https://doi.org/10.5194/hess-21-4973-2017>.
- Kääb, A., Berthier, E., Nuth, C., Gardelle, J., Arnaud, Y., 2012. Contrasting patterns of early twenty-first-century glacier mass change in the Himalayas. *Nature*, 5–8. <https://doi.org/10.1038/nature11324>.

- Kajander, J., 1993. Methodological aspects on river cryophenology exemplified by a tricentennial break-up time series from Tornio. *Geophysica* 29, 73–95.
- Kaser, G., Fountain, A., Jansson, P., 2003. A manual for monitoring the mass balance of mountain glaciers. In: IHP-VI Technical Documents in Hydrology. Paris.
- Kaser, G., Grosshauser, M., Marzeion, B., 2010. Contribution potential of glaciers to water availability in different climate regimes. *Proc. Natl. Acad. Sci. U. S. A.* 107, 20223–20227. <https://doi.org/10.1073/pnas.1008162107>.
- Koboltschnig, G.R., Schöner, W., 2011. The relevance of glacier melt in the water cycle of the Alps: the example of Austria. *Hydrol. Earth Syst. Sci.* 15, 2039–2048. <https://doi.org/10.5194/hess-15-2039-2011>.
- Koch, F., Henkel, P., Appel, F., Schmid, L., Bach, H., Lamm, M., Prasch, M., Schweizer, J., Mauser, W., 2019. Retrieval of snow water equivalent, liquid water content, and snow height of dry and wet snow by combining GPS signal attenuation and time delay. *Water Resour. Res.* 55, 4465–4487. <https://doi.org/10.1029/2018WR024431>.
- Kolosov, R.R., Prokushkin, A.S., Pokrovsky, O.S., 2016. Major anion and cation fluxes from the Central Siberian Plateau watersheds with underlying permafrost. *IOP Conf. Ser. Earth Environ. Sci.* 48. <https://doi.org/10.1088/1755-1315/48/1/012018>.
- Kraaijenbrink, P.D.A., Bierkens, M.F.P., Lutz, A.F., Immerzeel, W.W., 2017. Impact of a global temperature rise of 1.5 degrees Celsius on Asia's glaciers. *Nature* 549, 257–260. <https://doi.org/10.1038/nature23878>.
- Krasting, J.P., Broccoli, A.J., Dixon, K.W., Lanzante, J.R., 2013. Future changes in northern hemisphere snowfall. *J. Clim.* 26, 7813–7828. <https://doi.org/10.1175/JCLI-D-12-00832.1>.
- Kuhn, M., Batlogg, N., 1998. Glacier runoff in Alpine headwaters in a changing climate. In: *Hydrology, Water Resources and Ecology in Headwaters (Proceedings of the HeadWater'98 Conference Held at Meran/Merano, Italy, April 1998)*. IAHS Publ. No. 248, pp. 79–88.
- Kuusisto, E., 1980. On the values and variability of degree-day melting factor in Finland. *Nord. Hydrol.* 11, 235–242.
- Lambrecht, A., Mayer, C., 2009. Temporal variability of the non-steady contribution from glaciers to water discharge in western Austria. *J. Hydrol.* 376, 353–361. <https://doi.org/10.1016/j.jhydrol.2009.07.045>.
- Lang, H., 1986. Forecasting meltwater runoff from snow-covered areas and from glacier basins. In: Kraijenhoff, D. A., Moll, J.R. (Eds.), *River Flow Modelling and Forecasting Water Science and Technology Library, Volume 3*. Springer, Netherlands, pp. 99–127.
- Laudon, H., Sjöblom, V., Buffam, I., Seibert, J., Mört, M., 2007. The role of catchment scale and landscape characteristics for runoff generation of boreal streams. *J. Hydrol.* 344, 198–209. <https://doi.org/10.1016/j.jhydrol.2007.07.010>.
- Lehning, M., Löwe, H., Ryser, M., Raderschall, N., 2008. Inhomogeneous precipitation distribution and snow transport in steep terrain. *Water Resour. Res.* 44, 1–19. <https://doi.org/10.1029/2007WR006545>.
- Lemieux, J.M., Sudicky, E.A., Peltier, W.R., Tarasov, L., 2008. Dynamics of groundwater recharge and seepage over the Canadian landscape during the Wisconsinian glaciation. *J. Geophys. Res. Earth Surf.* 113, 1–18. <https://doi.org/10.1029/2007JF000838>.
- Lendzioch, T., Langhammer, J., Jenicek, M., 2019. Estimating snow depth and leaf area index based on UAV digital photogrammetry. *Sensors* 19, 1027. <https://doi.org/10.3390/s19051027>.
- Lindström, G., Johansson, B., Persson, M., Gardelin, M., Bergström, S., 1997. Development and test of the distributed HBV-96 hydrological model. *J. Hydrol.* 201, 272–288.
- Lindström, G., Bishop, K., Löfvenius, M.O., 2002. Soil frost and runoff at Svartberget, northern Sweden—measurements and model analysis. *Hydrol. Process.* 16, 3379–3392. <https://doi.org/10.1002/hyp.1106>.
- López-Moreno, J.I., Stähli, M., Lopezmoreno, J., Stahli, M., 2008. Statistical analysis of the snow cover variability in a subalpine watershed: assessing the role of topography and forest interactions. *J. Hydrol.* 348, 379–394. <https://doi.org/10.1016/j.jhydrol.2007.10.018>.
- López-Moreno, J.I., Revuelto, J., Fassnacht, S.R., Azorín-Molina, C., Vicente-Serrano, S.M., Morán-Tejeda, E., Sextone, G.A., 2015. Snowpack variability across various spatio-temporal resolutions. *Hydrol. Process.* 29, 1213–1224. <https://doi.org/10.1002/hyp.10245>.

- Luce, C.H., Tarboton, D.G., Cooley, K.R., 1998. The influence of the spatial distribution of snow on basin-averaged snowmelt. *Hydrol. Process.* 12, 1671–1683. [https://doi.org/10.1002/\(SICI\)1099-1085\(199808/09\)12:10/11<1671::AID-HYP688>3.0.CO;2-N](https://doi.org/10.1002/(SICI)1099-1085(199808/09)12:10/11<1671::AID-HYP688>3.0.CO;2-N).
- Lundberg, A., Richardson-Näslund, C., Andersson, C., 2006. Snow density variations: consequences for ground-penetrating radar. *Hydrol. Process.* 20, 1483–1495. <https://doi.org/10.1002/hyp.5944>.
- Lutz, A.F., Immerzeel, W.W., Shrestha, A.B., Bierkens, M.F.P., 2014. Consistent increase in high Asia's runoff due to increasing glacier melt and precipitation. *Nat. Clim. Chang.* 4, 587–592. <https://doi.org/10.1038/nclimate2237>.
- Lyon, S.W., Destouni, G., 2010. Changes in catchment-scale recession flow properties in response to permafrost thawing in the Yukon River Basin. *Int. J. Climatol.* 30, 2138–2145. <https://doi.org/10.1002/joc.1993>.
- Lyon, S.W., Destouni, G., Giesler, R., Humborg, C., Mört, M., Seibert, J., Karlsson, J., Troch, P.a., 2009. Estimation of permafrost thawing rates in a sub-arctic catchment using recession flow analysis. *Hydrol. Earth Syst. Sci. Discuss.* 6, 63–83. <https://doi.org/10.5194/hessd-6-63-2009>.
- Magnin, F., Haeberli, W., Linsbauer, A., Deline, P., Ravanel, L., 2020. Estimating glacier-bed overdeepenings as possible sites of future lakes in the de-glaciating Mont Blanc massif (Western European Alps). *Geomorphology* 350, 106913. <https://doi.org/10.1016/j.geomorph.2019.106913>.
- Magnuson, J.J., Robertson, D.M., Benson, B.J., Wynne, R.H., Livingstone, D.M., Arai, T., Assel, R.A., Barry, R.G., Card, V., Kuusisto, E., Granin, N.G., Prowse, T.D., Stewart, K.M., Vuglinski, V.S., 2000. Historical Trends in Lake and River Ice Cover in the Northern Hemisphere. *Science* 289, 1743–1746. <https://doi.org/10.1126/science.289.5485.1743>.
- Maidment, D.R., 1992. *Handbook of Hydrology*. McGraw-Hill Professional, New York.
- Malle, J., Rutter, N., Mazzotti, G., Jonas, T., 2019. Shading by trees and fractional snow cover control the sub-canopy radiation budget. *J. Geophys. Res. Atmos.* 124, 3195–3207. <https://doi.org/10.1029/2018JD029908>.
- Mankin, J.S., Viviroli, D., Singh, D., Hoekstra, A.Y., Diffenbaugh, N.S., 2015. The potential for snow to supply human water demand in the present and future. *Environ. Res. Lett.* 10. <https://doi.org/10.1088/1748-9326/10/11/114016>.
- Marks, D., Dozier, J., 1992. Climate and energy exchange at the snow surface in the Alpine Region of the Sierra Nevada: 2. Snow cover energy balance. *Water Resour. Res.* 28, 3043–3054. <https://doi.org/10.1029/92WR01483>.
- Martinec, J., 1975. Snowmelt—runoff model for stream flow forecasts. *Nord. Hydrol.* 6, 145–154. <https://doi.org/10.2166/nh.1975.010>.
- McCabe, M.F., Rodell, M., Alsdorf, D.E., Miralles, D.G., Uijlenhoet, R., Wagner, W., Lucieer, A., Houborg, R., Verhoest, N.E.C., Franz, T.E., Shi, J., Gao, H., Wood, E.F., 2017. The future of earth observation in hydrology. *Hydrol. Earth Syst. Sci.* 21, 3879–3914. <https://doi.org/10.5194/hess-21-3879-2017>.
- Meier, M.F., Tangborn, W.V., 1961. Distinctive characteristics of glacier runoff. *US Geol. Surv. Prof. Pap.* 424-B, 14–16.
- Miles, K.E., Hubbard, B., Quincey, D.J., Miles, E.S., Irvine-Fynn, T.D.L., Rowan, A.V., 2019. Surface and subsurface hydrology of debris-covered Khumbu Glacier, Nepal, revealed by dye tracing. *Earth Planet. Sci. Lett.* 513, 176–186. <https://doi.org/10.1016/j.epsl.2019.02.020>.
- Molotch, N.P., Margulis, S.A., 2008. Estimating the distribution of snow water equivalent using remotely sensed snow cover data and a spatially distributed snowmelt model: a multi-resolution, multi-sensor comparison. *Adv. Water Resour.* 31, 1503–1514. <https://doi.org/10.1016/j.advwatres.2008.07.017>.
- Musselman, K.N., Clark, M.P., Liu, C., Ikeda, K., Rasmussen, R., 2017. Slower snowmelt in a warmer world. *Nat. Clim. Chang.* 7, 214–219. <https://doi.org/10.1038/nclimate3225>.
- Musselman, K.N., Lehner, F., Ikeda, K., Clark, M.P., Prein, A.F., Liu, C., Barlage, M., Rasmussen, R., 2018. Projected increases and shifts in rain-on-snow flood risk over western North America. *Nat. Clim. Chang.* 8, 808–812. <https://doi.org/10.1038/s41558-018-0236-4>.
- Naegeli, K., Huss, M., Hoelzle, M., 2019. Change detection of bare-ice albedo in the Swiss Alps. *Cryosphere* 13, 397–412. <https://doi.org/10.5194/tc-13-397-2019>.

- Neal, E.G., Hood, E., Smikrud, K., 2010. Contribution of glacier runoff to freshwater discharge into the Gulf of Alaska. *Geophys. Res. Lett.* 37, 1–5. <https://doi.org/10.1029/2010GL042385>.
- Ohmura, A., 2001. Physical basis for the temperature-based melt-index method. *J. Appl. Meteorol.* 40, 753–761. [https://doi.org/10.1175/1520-0450\(2001\)040<0753:PBFTTB>2.0.CO;2](https://doi.org/10.1175/1520-0450(2001)040<0753:PBFTTB>2.0.CO;2).
- Østrem, G., Stanley, A., 1969. *Glacier Mass-balance Measurements: A Manual for Field and Office Work*. Canadian Department of Energy, Mines and Resources.
- Painter, T.H., Berisford, D.F., Boardman, J.W., Bormann, K.J., Deems, J.S., Gehrke, F., Hedrick, A., Joyce, M., Laidlaw, R., Marks, D., Mattmann, C., McGurk, B., Ramirez, P., Richardson, M., Skiles, S.M.K., Seidel, F.C., Winstral, A., 2016. The airborne snow observatory: fusion of scanning lidar, imaging spectrometer, and physically-based modeling for mapping snow water equivalent and snow albedo. *Remote Sens. Environ.* 184, 139–152. <https://doi.org/10.1016/j.rse.2016.06.018>.
- Paul, F., Haeberli, W., 2008. Spatial variability of glacier elevation changes in the Swiss Alps obtained from two digital elevation models. *Geophys. Res. Lett.* 35, 1–5. <https://doi.org/10.1029/2008GL034718>.
- Peck, E.L., Bissell, V.C., Jones, E.B., Burge, D.L., 1971. Evaluation of snow water equivalent by airborne measurement of passive terrestrial gamma radiation. *Water Resour. Res.* 7, 1151–1159.
- Pellicciotti, F., Brock, B., Strasser, U., Burlando, P., Funk, M., Corripio, J., 2005. An enhanced temperature-index glacier melt model including the shortwave radiation balance: development and testing for Haut Glacier d’Arolla, Switzerland. *J. Glaciol.* 51, 573–587. <https://doi.org/10.3189/172756505781829124>.
- Pohl, S., Marsh, P., Liston, G.E., 2006. Spatial-temporal variability in turbulent fluxes during spring snowmelt. *Arct. Antarct. Alp. Res.* 38, 136–146. [https://doi.org/10.1657/1523-0430\(2006\)038\[0136:SVITFD\]2.0.CO;2](https://doi.org/10.1657/1523-0430(2006)038[0136:SVITFD]2.0.CO;2).
- Pritchard, H.D., 2019. Asia’s shrinking glaciers protect large populations from drought stress. *Nature* 569, 649–654. <https://doi.org/10.1038/s41586-019-1240-1>.
- Prokop, A., 2008. Assessing the applicability of terrestrial laser scanning for spatial snow depth measurements. *Cold Reg. Sci. Technol.* 54, 155–163. <https://doi.org/10.1016/j.coldregions.2008.07.002>.
- Prowse, T.D., 2005. River-ice hydrology. In: Anderson, M.G. (Ed.), *Encyclopedia of Hydrological Sciences*. John Wiley and Sons, Chichester, UK, pp. 1–21.
- Prowse, T., Carter, T., 2002. Significance of ice-induced storage to spring runoff: a case study of the Mackenzie River. *Hydrol. Process.* 16, 779–788. <https://doi.org/10.1002/hyp.371>.
- Racoviteanu, A.E., Armstrong, R., Williams, M.W., 2013. Evaluation of an ice ablation model to estimate the contribution of melting glacier ice to annual discharge in the Nepal Himalaya. *Water Resour. Res.* 49, 5117–5133. <https://doi.org/10.1002/wrcr.20370>.
- Radić, V., Hock, R., 2014. Glaciers in the Earth’s hydrological cycle: assessments of glacier mass and runoff changes on global and regional scales. *Surv. Geophys.* 35, 813–837. <https://doi.org/10.1007/s10712-013-9262-y>.
- Rannie, W.F., 1983. Breakup and freezeup of the Red River at Winnipeg, Manitoba Canada in the 19th century and some climatic implications. *Clim. Chang.* 5, 283–296.
- Rasmussen, R., Baker, B., Kochendorfer, J., Meyers, T., Landolt, S., Fischer, A.P., Black, J., Thériault, J.M., Kucera, P., Gochis, D., Smith, C., Nitu, R., Hall, M., Ikeda, K., Gutmann, E., 2012. How well are we measuring snow: the NOAA/FAA/NCAR winter precipitation test bed. *Bull. Am. Meteorol. Soc.* 93, 811–829. <https://doi.org/10.1175/BAMS-D-11-00052.1>.
- Revuelto, J., Jonas, T., López-Moreno, J.-I., 2016. Backward snow depth reconstruction at high spatial resolution based on time-lapse photography. *Hydrol. Process.* <https://doi.org/10.1002/hyp.10823>. n/a-n/a.
- Rogger, M., Chirico, G.B., Hausmann, H., Krainer, K., Brückl, E., Stadler, P., Blöschl, G., 2017. Impact of mountain permafrost on flow path and runoff response in a high alpine catchment. *Water Resour. Res.* 53, 1288–1308. <https://doi.org/10.1002/2016WR019341>.
- Roth, T.R., Nolin, A.W., 2017. Forest impacts on snow accumulation and ablation across an elevation gradient in a temperate montane environment. *Hydrol. Earth Syst. Sci.* 21, 5427–5442. <https://doi.org/10.5194/hess-21-5427-2017>.

- Röthlisberger, H., Lang, H., 1987. Glacial hydrology. In: Gurnell, M., Clark, M.J. (Eds.), *Glacio-Fluvial Sediment Transfer: An Alpine Perspective*. John Wiley & Sons, Ltd, Chichester, UK, pp. 207–284.
- Rücker, A., Boss, S., Kirchner, J.W., von Freyberg, J., 2019. Monitoring snowpack outflow volumes and their isotopic composition to better understand streamflow generation during rain-on-snow events. *Hydrol. Earth Syst. Sci.* 23, 2983–3005. <https://doi.org/10.5194/hess-23-2983-2019>.
- Schaefli, B., Hingray, B., Musy, A., 2007. Climate change and hydropower production in the Swiss Alps: quantification of potential impacts and related modelling uncertainties. *Hydrol. Earth Syst. Sci.* 11, 1191–1205.
- Schaefli, B., Manso, P., Fischer, M., Huss, M., Farinotti, D., 2019. The role of glacier retreat for Swiss hydropower production. *Renew. Energy* 132, 615–627. <https://doi.org/10.1016/j.renene.2018.07.104>.
- Schelker, J., Kuglerová, L., Eklöf, K., Bishop, K., Laudon, H., 2013. Hydrological effects of clear-cutting in a boreal forest—snowpack dynamics, snowmelt and streamflow responses. *J. Hydrol.* 484, 105–114. <https://doi.org/10.1016/j.jhydrol.2013.01.015>.
- Schoof, C., 2010. Ice-sheet acceleration driven by melt supply variability. *Nature* 468, 803–806. <https://doi.org/10.1038/nature09618>.
- Schweizer, J., Bartelt, P., van Herwijnen, A., 2021. Snow avalanches. In: Haeberli, W., Whiteman, C. (Eds.), *Snow and Ice-Related Hazards, Risks and Disasters*. Elsevier, pp. 377–416.
- Seibert, J., 1999. Regionalisation of parameters for a conceptual rainfall-runoff model. *Agric. For. Meteorol.* 98–99, 279–293.
- Seibert, J., Vis, M., Kohn, I., Weiler, M., Stahl, K., 2018. Technical note: representing glacier geometry changes in a semi-distributed hydrological model. *Hydrol. Earth Syst. Sci.* 22. <https://doi.org/10.5194/hess-22-2211-2018>.
- Seidel, K., Martinec, J., 2010. *Remote Sensing in Snow Hydrology—Runoff Modelling*. Springer Verlag, Effect of Climate Change.
- Sevruk, B., Ondráš, M., Chvíla, B., 2009. The WMO precipitation measurement intercomparisons. *Atmos. Res.* 92, 376–380. <https://doi.org/10.1016/j.atmosres.2009.01.016>.
- Shanley, J.B., Chalmers, A., 1999. The effect of frozen soil on snowmelt runoff at Sleepers River, Vermont. *Hydrol. Process.* 13, 1843–1857. [https://doi.org/10.1002/\(SICI\)1099-1085\(199909\)13:12/13<1843::AID-HYP879>3.0.CO;2-G](https://doi.org/10.1002/(SICI)1099-1085(199909)13:12/13<1843::AID-HYP879>3.0.CO;2-G).
- Shean, D.E., Bhushan, S., Montesano, P., Rounce, D.R., Arendt, A., Osmanoglu, B., 2020. A systematic, regional assessment of high mountain Asia Glacier mass balance. *Front. Earth Sci.* 7, 1–19. <https://doi.org/10.3389/feart.2019.00363>.
- Sicart, J.E., Hock, R., Six, D., 2008. Glacier melt, air temperature, and energy balance in different climates: the Bolivian Tropics, the French Alps, and northern Sweden. *J. Geophys. Res. Atmos.* 113, 1–11. <https://doi.org/10.1029/2008JD010406>.
- Singh, P., Singh, V.P., 2001. *Snow and Glacier Hydrology*. Kluwer Academic Publishers, London.
- Smyth, E.J., Raleigh, M.S., Small, E.E., 2019. Particle filter data assimilation of monthly snow depth observations improves estimation of snow density and SWE. *Water Resour. Res.*, 1296–1311. <https://doi.org/10.1029/2018WR023400>.
- Sold, L., Huss, M., Hoelzle, M., Anderegg, H., Joerg, P.C., Zemp, M., 2013. Methodological approaches to infer end-of-winter snow distribution on alpine glaciers. *J. Glaciol.* 59, 1047–1059. <https://doi.org/10.3189/2013JoG13J015>.
- Sorg, A., Bolch, T., Stoffel, M., Solomina, O., Beniston, M., 2012. Climate change impacts on glaciers and runoff in Tien Shan (Central Asia). *Nat. Clim. Chang.* 2, 725–731. <https://doi.org/10.1038/NCLIMATE1592>.
- Stahl, K., Moore, R.D., Shea, J.M., Hutchinson, D., Cannon, A.J., 2008. Coupled modelling of glacier and streamflow response to future climate scenarios. *Water Resour. Res.* 44, 1–13. <https://doi.org/10.1029/2007WR005956>.
- Stahl, K., Weiler, M., Kohn, I., Seibert, J., Vis, M., Gerlinger, K., 2017. The snow and glacier melt components of streamflow of the river Rhine and its tributaries considering the influence of climate change. In: Final report to the International Commission for the Hydrology of the Rhine Basin (CHR).

- Stähli, M., Gustafsson, D., 2006. Long-term investigations of the snow cover in a subalpine semi-forested catchment. *Hydrol. Process.* 20, 411–428. <https://doi.org/10.1002/hyp.6058>.
- Stähli, M., Jansson, P.-E., Lundin, L.-C., 1996. Preferential water flow in a frozen soil—a two-domain model approach. *Hydrol. Process.* 10, 1305–1316.
- Stähli, M., Jansson, P.-E., Lundin, L.-C., 1999. Soil moisture redistribution and infiltration in frozen sandy soils. *Water Resour. Res.* 35, 95–103.
- Stähli, M., Nyberg, L., Mellander, P.-E., Jansson, P.-E., Bishop, K.H., 2001. Soil frost effects on soil water and runoff dynamics along a boreal transect: 2. Simulations. *Hydrol. Process.* 15, 927–941. <https://doi.org/10.1002/hyp.232>.
- Stenborg, T., 1970. Delay of Run-Off from a Glacier Basin. *Geogr. Ann. Ser. A, Phys. Geogr.* 52, 1–30.
- Storvold, R., Malnes, E., Larsen, Y., Høgda, K.A., Hamran, S.E., Müller, K., Langley, K.A., 2006. Sar remote sensing of snow parameters in Norwegian areas—current status and future perspective. *J. Electromagn. Waves Appl.* 20, 1751–1759. <https://doi.org/10.1163/156939306779292192>.
- Streltsiky, D., 2021. Permafrost degradation. In: Haeberli, W., Whiteman, C. (Eds.), *Snow and Ice-Related Hazards, Risks and Disasters*. Elsevier, pp. 297–322.
- Surfleet, C.G., Tullos, D., 2013. Variability in effect of climate change on rain-on-snow peak flow events in a temperate climate. *J. Hydrol.* 479, 24–34. <https://doi.org/10.1016/j.jhydrol.2012.11.021>.
- Tait, A.B., 1998. Estimation of snow water equivalent using passive microwave radiation data. *Remote Sens. Environ.* 64, 286–291. [https://doi.org/10.1016/S0034-4257\(98\)00005-4](https://doi.org/10.1016/S0034-4257(98)00005-4).
- Taylor, S., Feng, X., Kirchner, J.W., Osterhuber, R., Klaue, B., Renshaw, C.E., 2001. Isotopic evolution of a seasonal snowpack and its melt. *Water Resour. Res.* 37, 759–769.
- Techel, F., Pielmeier, C., 2011. Point observations of liquid water content in wet snow—investigating methodical, spatial and temporal aspects. *Cryosphere* 5, 405–418. <https://doi.org/10.5194/tc-5-405-2011>.
- Van Tiel, M., Teuling, A.J., Wanders, N., Vis, M.J.P., Stahl, K., Van Loon, A.F., 2018. The role of glacier changes and threshold definition in the characterisation of future streamflow droughts in glacierised catchments. *Hydrol. Earth Syst. Sci.* 22, 463–485. <https://doi.org/10.5194/hess-22-463-2018>.
- Vander Jagt, B.J., Durand, M.T., Margulis, S.A., Kim, E.J., Molotch, N.P., 2013. The effect of spatial variability on the sensitivity of passive microwave measurements to snow water equivalent. *Remote Sens. Environ.* 136, 163–179. <https://doi.org/10.1016/j.rse.2013.05.002>.
- Vincent, A., Violette, S., Aðalgeirsdóttir, G., 2019. Groundwater in catchments headed by temperate glaciers: a review. *Earth Sci. Rev.* 188, 59–76. <https://doi.org/10.1016/j.earscirev.2018.10.017>.
- Viviroli, D., Weingartner, R., 2004. The hydrological significance of mountains: from regional to global scale. *Hydrol. Earth Syst. Sci.* 8, 1017–1030. <https://doi.org/10.5194/hess-8-1017-2004>.
- Wachter, K., 2007. *The Analysis of the Danube Floods 2006*. ICPDR—International Commission for the Protection of the Danube River, Vienna.
- Walvoord, M.A., Striegl, R.G., 2007. Increased groundwater to stream discharge from permafrost thawing in the Yukon River basin: potential impacts on lateral export of carbon and nitrogen. *Geophys. Res. Lett.* 34. <https://doi.org/10.1029/2007GL030216>.
- Wanders, N., Wada, Y., Van Lanen, H.A.J., 2015. Global hydrological droughts in the 21st century under a changing hydrological regime. *Earth Syst. Dyn.* 6, 1–15. <https://doi.org/10.5194/esd-6-1-2015>.
- Weber, M., Braun, L., Mauser, W., Prasch, M., 2010. Contribution of rain, snow-and icemelt in the upper Danube discharge today and in the future. *Geogr. Fis. Din. Quat.* 33, 221–230.
- Weingartner, R., Aschwanden, H., 1992. Abflussregimes als Grundlage zur Abschätzung von Mittelwerten des Abflusses. In: Federal Office for the Environment (Ed.), *Hydrologischer Atlas der Schweiz*. FOEN, Bern. Tafel 5.2.
- Werder, M.A., Funk, M., 2009. Dye tracing a jökulhlaup : II. Testing a jokulhlaup model against flow speeds inferred from measurements. *J. Glaciol.* 55, 899–908.

- Wever, N., Jonas, T., Fierz, C., Lehning, M., 2014. Model simulations of the modulating effect of the snow cover in a rain-on-snow event. *Hydrol. Earth Syst. Sci.* 18, 4657–4669. <https://doi.org/10.5194/hess-18-4657-2014>.
- Woo, M.-K., Kane, D.L., Carey, S.K., Yang, D., 2008. Progress in permafrost hydrology in the New Millennium. *Permafrost. Periglac. Process.* 19, 237–254. <https://doi.org/10.1002/ppp.613>.
- Wouters, B., Gardner, A.S., Moholdt, G., 2019. Global glacier mass loss during the GRACE satellite mission (2002–2016). *Front. Earth Sci.* 7, 1–11. <https://doi.org/10.3389/feart.2019.00096>.
- Wu, W.Y., Lan, C.W., Lo, M.H., Reager, J.T., Famiglietti, J.S., 2015. Increases in the annual range of soil water storage at northern middle and high latitudes under global warming. *Geophys. Res. Lett.* 42, 3903–3910. <https://doi.org/10.1002/2015GL064110>.
- Würzer, S., Jonas, T., 2018. Spatio-temporal aspects of snowpack runoff formation during rain on snow. *Hydrol. Process.* 32, 3434–3445. <https://doi.org/10.1002/hyp.13240>.
- Würzer, S., Jonas, T., Wever, N., Lehning, M., 2016. Influence of initial snowpack properties on runoff formation during rain-on-snow events. *J. Hydrometeorol.* 17, 1801–1815. <https://doi.org/10.1175/JHM-D-15-0181.1>.
- Zappa, M., Kan, C., 2007. Extreme heat and runoff extremes in the Swiss Alps. *Nat. Hazards Earth Syst. Sci.* 7, 375–389. <https://doi.org/10.5194/nhess-7-375-2007>.
- Zemp, M., Thibert, E., Huss, M., Stumm, D., Rolstad Denby, C., Nuth, C., Nussbaumer, S.U., Moholdt, G., Mercer, A., Mayer, C., Joerg, P.C., Jansson, P., Hynek, B., Fischer, A., Escher-Vetter, H., Elvehøy, H., Andreassen, L.M., 2013. Reanalysing glacier mass balance measurement series. *Cryosphere* 7, 1227–1245. <https://doi.org/10.5194/tc-7-1227-2013>.
- Zemp, M., Huss, M., Thibert, E., Eckert, N., McNabb, R., Huber, J., Barandun, M., Machguth, H., Nussbaumer, S.U., Gärtner-Roer, I., Thomson, L., Paul, F., Maussion, F., Kutuzov, S., Cogley, J.G., 2019. Global glacier mass changes and their contributions to sea-level rise from 1961 to 2016. *Nature* 568, 382–386. <https://doi.org/10.1038/s41586-019-1071-0>.